Smart Nanozymes for Cancer Therapy: The Next Frontier in Oncology

Navya P. N., Sunil Mehla, Amrin Begum, Harit K. Chaturvedi, Ruchika Ojha, Christian Hartinger, Magdalena Plebanski, and Suresh K. Bhargava*

Nanomaterials that mimic the catalytic activity of natural enzymes in the complex biological environment of the human body are called nanozymes. Recently, nanozyme systems have been reported with diagnostic, imaging, and/or therapeutic capabilities. Smart nanozymes strategically exploit the tumor microenvironment (TME) by the in situ generation of reactive species or by the modulation of the TME itself to result in effective cancer therapy. This topical review focuses on such smart nanozymes for cancer diagnosis, and therapy modalities with enhanced therapeutic effects. The dominant factors that guide the rational design and synthesis of nanozymes for cancer therapy include an understanding of the dynamic TME, structure-activity relationships, surface chemistry for imparting selectivity, and site-specific therapy, and stimulus-responsive modulation of nanozyme activity. This article presents a comprehensive analysis of the subject including the diverse catalytic mechanisms of different types of nanozyme systems, an overview of the TME, cancer diagnosis, and synergistic cancer therapies. The strategic application of nanozymes in cancer treatment can well be a game changer in future oncology. Moreover, recent developments may pave the way for the deployment of nanozyme therapy into other complex healthcare challenges, such as genetic diseases, immune disorders, and ageing.

1. Introduction

According to the World Health Organization, cancer is currently the leading cause of death worldwide and accounted for nearly 10 million deaths in 2020.[1] Cancer-related mortality is expected to rise to 13.1 million every year by 2030.[2] Many types of cancers can be treated effectively and potentially cured if diagnosed early. However, cancer is extremely difficult to manage in the later stages because of the probability of recurrence and the possibility of spreading to other parts of the body.[3] For instance, 16% of patients with second or higher-stage renal cancer do not survive, whereas the survival rate for early-stage renal cancer patients was estimated to be as high as 99%.[4] For patients with epithelial ovarian cancer, the 5-year relative survival rate is 29% for late-stage presentation, whilst for the early-stage disease, it is 92%.[5] Thus, in dealing with high-fatality diseases such as cancer, early diagnosis is often the key to survival. Moreover, most traditional treatment modalities often prove insufficient in the efficient management of cancer, given cancer cells develop drug-resistance and undesired side effects such as myelosuppression and kidney damage.[6] Thus, developing novel chemotherapeutics to combat cancer garners significant attention and is regularly classified as a priority research area.

Akin to other fields of research, nanotechnology has been enthusiastically pursued for diagnosis and treatment of cancer. Nanomaterials exhibit large surface areas, high reactivity, sensitivity and specificity, and intrinsic catalytic ability to generate

N. P. N., S. Mehla, A. Begum, R. Ojha, S. K. Bhargava
Centre for Advanced Materials and Industrial Chemistry
School of Science
STEM College
RMIT University
Melbourne 3000, Australia
E-mail: suresh.bhargava@rmit.edu.au

H. K. Chaturvedi
Head Surgical Oncologist
Max Institute of Cancer Care
Delhi 110024, India

C. Hartinger
School of Chemical Sciences
The University of Auckland
Auckland 1142, Private Bag 92019, New Zealand

M. Plebanski
Cancer, Ageing and Vaccines Research Group
School of Health and Biomedical Sciences
STEM College
RMIT University
Melbourne 3000, Australia

ADVANCED
SCIENCE NEWS
www.advancedsciencenews.com

ADVANCED
HEALTHCARE
MATERIALS
www.advhealthmat.de
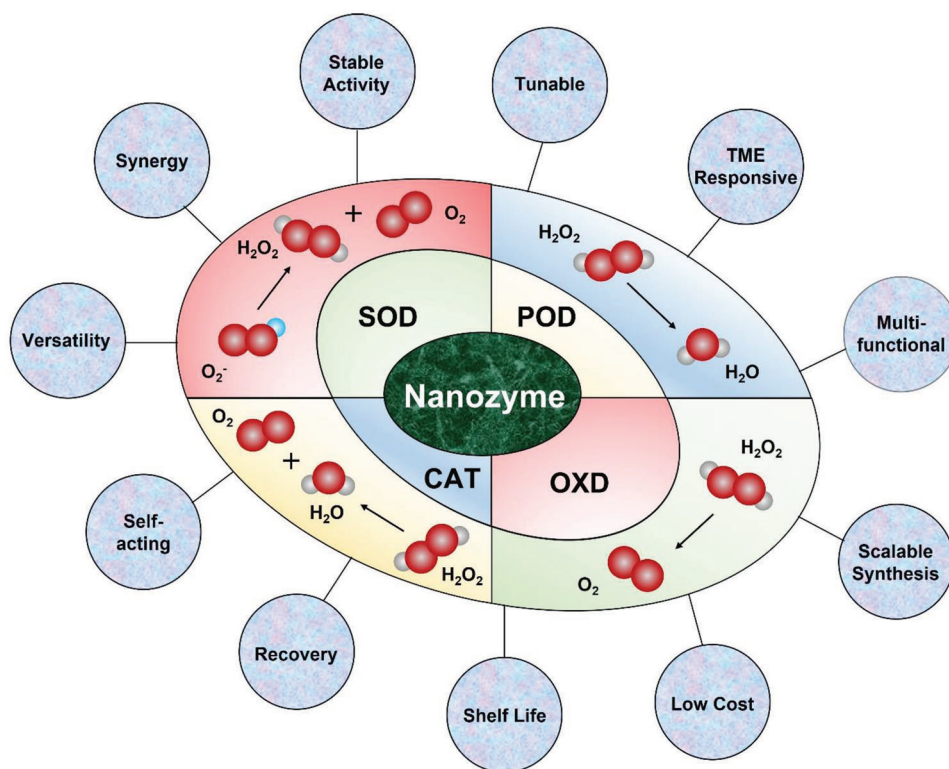
Figure 1. Schematic representation of the desirable characteristics of novel nanozymes for cancer theranostics, and enzymatic reactions exhibited by four common types of nanozymes, that is, catalase (CAT)-, superoxide dismutase (SOD)-, peroxidase (POD)- and oxidase (OXD)-mimicking nanozymes.

and scavenge ROS. For instance, metal nanoparticles, metal oxide nanocomposites, and carbon-based nanomaterials have been used for molecular detection[7] and treatment of several diseases.[8] Thus, the term nanozyme was coined to represent a new class of nanomaterials that exhibit enzyme-like activities. Nanozymes are nanomaterials that mimic the catalytic activities of natural enzymes and have the capability to overcome the limitations of natural enzymes.[9] Some common natural enzymes whose biocatalytic activities have been successfully mimicked by nanomaterials include peroxidase, catalase, superoxide dismutase, oxidase, and phosphatase.[10] Nanozymes exhibit several advantages over natural enzymes, such as high stability, ease of synthesis, recyclability, tunable catalytic activity, and applicability to various health problems.[11]

Nanozymes have significant potential as efficient therapeutic agents for cancer remediation because of their capability to regulate the redox level of cells and their synergistic catalytic activity in the dynamic TME.[12] ROS are the by-products of oxygen metabolism in cells and are generated in the human body through the action of natural enzymes. ROS in the human body mainly refers to singlet oxygen, superoxide, peroxide radicals, and oxygen-containing radicals. An abnormal rise in ROS levels disturbs homeostasis and causes oxidative stress in cells. Thus, nanozymes with high catalytic activities can control the intracellular and extracellular ROS levels to impact tumor cell apoptosis.[13] For instance, catalase- and superoxide dismutase-mimicking nanozymes were reported to efficiently regulate intracellular ROS levels, which protected the cells from oxidative damage.[12] In contrast, oxidase- and peroxidase-

mimicking nanozymes induced extracellular ROS production and promoted apoptosis in cancer cells.[14] Notably, the TME plays a critical role in controlling the propagation and colonization of cancer cells in other parts of the body.[15] The TME characteristics such as hypoxia, acidity, and overproduced hydrogen peroxide (H_2O_2) drastically reduce the therapeutic effects of cancer drugs and also can promote tumor proliferation and metastasis. Thus, substantial research efforts have been focused on developing nanozymes that can overcome the diversity of outcomes from therapy posed by the nature of the TME to enable better patient outcomes.[16] **Figure 1** schematically depicts the four most common types of nanozymes, their catalytic action, and the ideal characteristics desired from novel nanozymes.

This review is divided into eight sections. After an introduction to the topic in Section 1, Section 2 describes the different types of nanozymes and their catalytic mechanisms. Section 3 provides a very brief overview of the design and synthesis of different types of nanozymes while the tumor microenvironment and its importance in development of cancer therapies is elaborated in Section 4 where the challenges and opportunities presented by the dynamic TME are also analyzed. Section 5 is focused on the recent developments in the use of nanozymes for cancer diagnosis. Smart nanozymes-driven cancer therapy achieved through reactive oxygen species generation or hypoxia relief is elaborated in detail in Section 6. Section 7 reports on the progress of nanozymes-driven cancer therapies in clinical trials. Conclusions, challenges, and authors' perspective are presented in Section 8. A brief overview of biomarker testing for cancer diagnosis

**ADVANCED
SCIENCE NEWS**

www.advancedsciencenews.com

**ADVANCED
HEALTHCARE
MATERIALS**

www.advhealthmat.de

Table 1. Examples of different nanozyme-driven cancer therapy approaches.

Enzyme-like activity	Nanozyme formulation	Therapy	Tumor model	Reference
CAT-like activity	MnTCPP–Hf–FA MOFNPs	Radiotherapy	B16-F10 melanoma model	[19]
	Bi_2Se_3–MnO_2@BSA	Radiotherapy	Female BALB/c mice with 4T1 cells	[20]
	Cu_2MoS_4 (CMS)/Au	Phototherapy-induced immunotherapy	U14 tumor-bearing mice	[21]
	FA-Fht	Radiotherapy	CT26 cells in BALB/c mice	[22]
	Pt@Au-Ce6/Res-Lip	Trimodal therapeutic modality (chemotherapy, photothermal therapy (PTT), and photodynamic therapy (PDT))	Female Kunming mice with U14 tumor cells	[23]
	IrO_2@MSN@PDA-BSA(Ce6)	Combined PDT and PTT	HT29 cells with BALB/c mice	[24]
	Dox@MOF-Au-PEG	Radiochemotherapy	U87MG tumor-bearing nude mice	[25]
	PCN-224-Pt	PDT	H22 tumor-bearing mice	[26]
	PLGA/DOX@PDA-Au-PEG NPs	Chemo-photothermal therapy	BALB/c mice bearing subcutaneous 4T1 tumors	[27]
	Pd@TiO_2	PDT and PTT	4T1 tumor-bearing mice	[28]
	Fe_3O_4/Pt-FLU@PEG	Catalytic tumor therapy	4T1 tumor-bearing mice	[29]
POD-like activity	CuS/HSA-TAPP	Sonodynamic therapy (SDT) and PTT	MCF-7 tumor-bearing BALB/c mice	[30]
	MnPcNPs	Catalytic tumor therapy	HeLa tumor-bearing mouse model	[31]
	GQD-SPNs	Catalytic tumor therapy	HeLa tumor-bearing mouse model	[32]
	BSA-capped F-BSP NCs	Phototherapy	Mice with HeLa cells	[33]
	$SnFe_2O_4$	PTT, PDT, and chemodynamic therapy (CDT)	Female Balb/c nude mice with 4T1 breast tumors	[34]
SOD/POD/CAT-like activity	FePOs	Catalytic tumor therapy	Female Balb/c nude mice with 4T1 breast tumors	[35]
	PHMZCO-AT	Nanozyme-initiated chemodynamic therapy	4T1 tumor-bearing mice	[36]
GOD/POD-like activity	DMSN-Au-Fe_3O_4 NPs	Nanocatalytic tumor-specific therapy	4T1 breast tumor xenograft on nude mice	[37]
OXD-like activity	Palladium concave nanocrystals	Ascorbate based antitumor therapy	Mice bearing human colorectal carcinoma HCT116 tumor xenografts	[38]
NOX/SOD-like activity	Pt-MIL-101	Ferroptosis-induced tumor therapy	Xenograft murine breast cancer model of BALB/c mice	[39]
SOD/CAT/POD/GSHOD-like activity	Fe_3O_4/Ag/Bi_2MoO_6 nanoparticle	PDT/PTT/CDT	4T1 tumor-bearing Balb/c mice	[40]
POD-like activity	Co-Fc@GOx	CDT	4T1 tumor-bearing mice	[41]
OXD-like activity	DOX@HMSN/Mn_3O_4(R)	Radio-/chemotherapy	Male C57BL mice with A375 cells	[42]
CAT/GOx-like activity	P@Pt@P–Au–FA	Catalytic cascade-enhanced synergistic cancer therapy	4T1 tumor-bearing mice	[43]

and different types of conventional and emerging cancer therapies are provided in the Supporting Information.

2. Different Types of Nanozymes and Their Modes of Operation

A number of nanozymes have been reported with high enzymatic activities and significant potential for use in cancer treatment.[17] The catalytic activity of nanozymes and their effectiveness in biomedical applications are strongly governed by their physicochemical properties.[11] Natural enzymes can be classified into seven types based on their enzymatic action as oxidoreductase, transferases, hydrolases, lyases, isomerases, ligases, or translocases.[18] Most nanozymes, especially, the ones with demonstrated cancer theranostic activity, mimic the biocatalytic action of the oxidoreductase family of natural enzymes. A list of

different types of nanozyme-mediated cancer therapies classified according to the parent enzyme type is presented in **Table 1**.[19–43] The oxidoreductases mimicking nanozymes that have been explored for their use in cancer therapy include the enzymes POD, OXD, CAT, and SOD as shown in Figure 1. Nanozymes' enzymatic activities can often be controlled through modulation of the pH, temperature, light, magnetic field, or other external stimuli, which can render them more effective in cancer treatment. This section describes different types of nanozymes and their modes of operation in biological environment, including the TME.

2.1. Peroxidase-Mimicking Nanozymes

Peroxidases are a class of enzymes that play a major role in breaking H_2O_2 into non-toxic products like water. The main

**ADVANCED
SCIENCE NEWS**

www.advancedsciencenews.com

**ADVANCED
HEALTHCARE
MATERIALS**

www.advhealthmat.de

chemical reaction of peroxidases typically involves the reduction of H_2O_2 and oxidation of an electron-donating substrate (Figure 1).[44] In the recent literature, a plethora of nanomaterials has been reported that exhibit intrinsic peroxidase-like activity. These include nanoparticles formed from Fe_3O_4, Co_3O_4, Cu_2O, CdS, FeS, FeSe, FeTe, CeO_2, $CoFe_2O_4$, $ZnFe_2O_4$, $MnFe_2O_4$, $BiFeO_3$, carbon nanotubes, graphene oxide, polypyrroles, or fullerenes.[45] The POD-like activity of any nanomaterial can be evaluated by measuring the concentration of H_2O_2 using a variety of chromogenic substrates such as hydroquinone, 1,2,3-trihydroxybenzene (THB), o-phenylenediamine (OPD), 2,2'-azino-bis-(3-ethylbenzothiozoline-6-sulfonic acid (ABTS), and 3,3',5,5'-tetramethylbenzidine (TMB). However, TMB is the most widely used substrate to investigate peroxidase mimicking activity due to its low carcinogenicity and high absorption coefficient of its reaction products. An example of the determination of the enzymatic kinetics for Fe_3O_4, carbon, and gold nanozymes using standardized chromogenic assays is depicted in **Figure 2**. The biocatalytic activity of the nanozymes strongly depends on the environment, such as pH, temperature, and the presence of other species, including metal ions and organic molecules. For instance, Li et al. developed carbon dots confined in N-doped carbon, which behaved like peroxidases in the colorimetric detection of D-amino acids, to aid in diagnosing patients with early gastric cancer.[46] Similarly, graphene quantum dots/semiconducting polymer nanocomposites showed enhanced peroxidase-like activity for tumor therapy through the photothermal effect.[32] A fluorescent nanozyme was also reported, which exhibited excellent peroxidase-like activity and proved effective in ROS-mediated tumor remediation without any damage to normal cells.[47] Albumin nanoparticles encapsulated Prussian blue nanoparticles also exhibited peroxidase activity and allowed successful detection of low levels of tumor marker prostate-specific antigen (PSA).[48]

2.2. Oxidase-Mimicking Nanozymes

Oxidase enzymes are a family of enzymes that catalyze redox reactions using dioxygen as an electron acceptor to produce water (H_2O) or H_2O_2 as by-products. Examples of natural enzymes that belong to the oxidase family include cytochrome c oxidase, glucose oxidase, monoamine oxidase, cytochrome P450 oxidase, NADPH oxidase, xanthine oxidase, L-gluconolactone oxidase, laccase, lysyl oxidase, polyphenol oxidase, and so on. Thus, each type of oxidase enzyme targets specific substrates. For instance, glucose oxidase catalyzes the conversion of β-D-glucose into gluconic acid and H_2O_2.[49]

Several nanomaterials exhibited catalytic activity for the oxidation of substrates like the natural oxidases.[50] Nanoceria is a commonly used oxidase nanozyme. Its oxidase activity is attributed to the redox switching between Ce^{3+} and Ce^{4+} oxidation states and the associated production of superoxide radicals.[51] Similarly, a variety of noble metal-based nanozymes with different capping and stabilizing agents exhibited oxidase activity.[52] An Mn-based semiconducting polymeric nanozyme with inherent oxidase activity was employed in acid-induced cancer therapy along with the capability for ratiometric near-infrared fluorescence (NIRF)-photoacoustic (PA) molecular imaging, which provided avenues for following in vivo anticancer efficacy of

the nanozymes.[53] Leveraging the magnetic properties of iron, an oxidase mimicking nanozyme was reported consisting of platinum nanoparticles grafted onto MIL-101 (Fe) framework for ferroptotic tumor therapy involving a catalytic cascade.[39] The nanozyme platform, DOX@HMSN/Mn_3O_4(R), was tested for the synergistic application of radio- and chemotherapy in mice. The DOX@HMSN/Mn_3O_4 nanozyme could effectively overproduce ROS when irradiated with X-ray and exhibited enhanced tumor-targeting and oxidase-like activity under radiotherapy conditions by producing high levels of O_2.[42] Similarly, inspired by the oxidative catalytic cascades driven by Co–Fe NMOF nanozyme was developed, which could effectively deliver glucose oxidase (GOx) and catalyze the conversion of endogenous glucose to gluconic acid and H_2O_2. The increase in the H_2O_2 content triggered a ROS burst that was observed to effectively destroy tumor cells.[41]
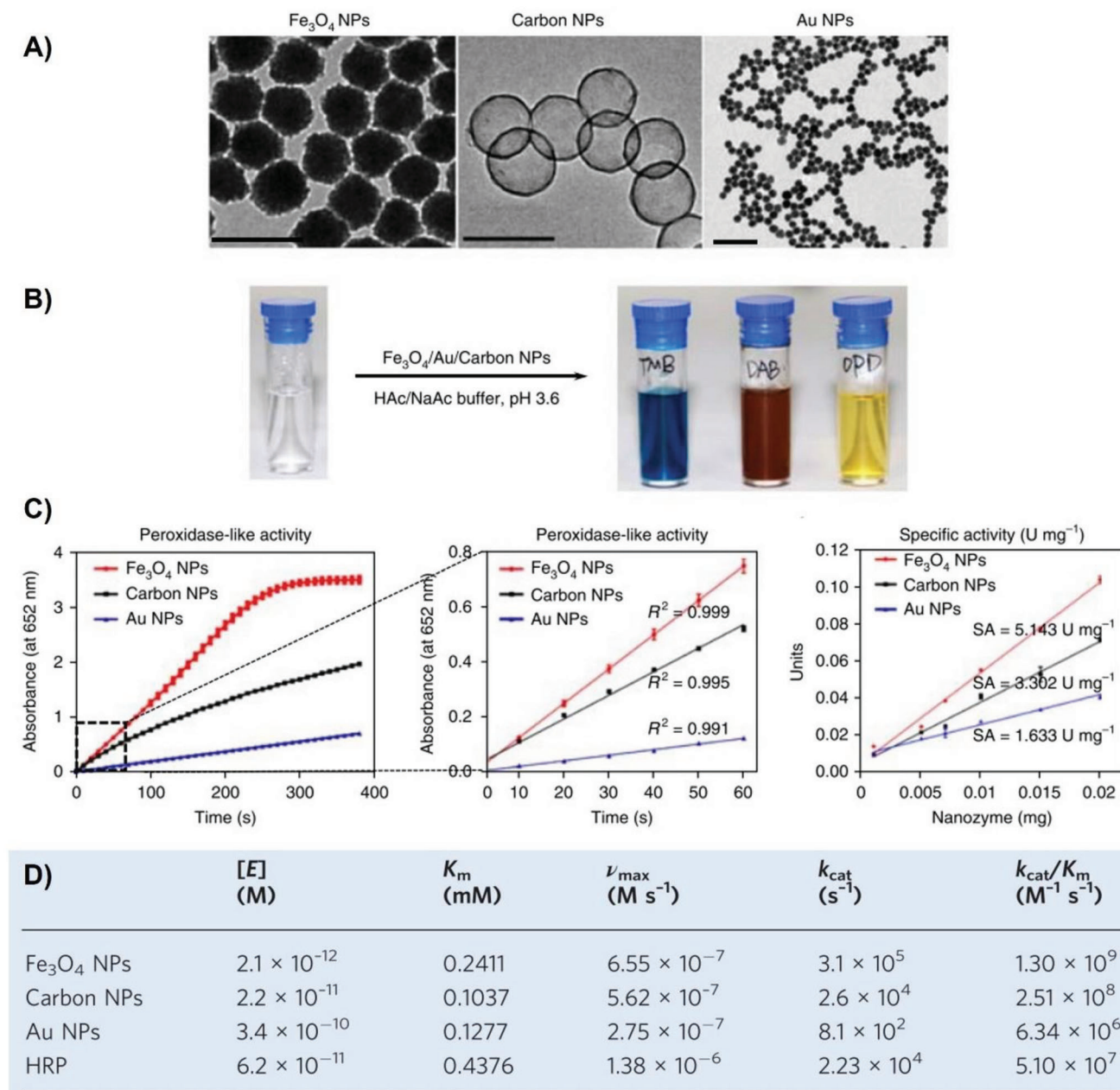
2.3. Superoxide Dismutase-Mimicking Nanozymes

Superoxide radicals are produced as a by-product of oxygen metabolism and their build-up can cause severe oxidative damage to normal cells.[54] Thus, superoxide radicals need to be regularly broken down into a harmless form of oxygen to avoid damage to normal cells.[55] SOD enzymes are highly efficient antioxidant enzymes that catalyze the conversion of superoxide radicals into oxygen and hydrogen peroxide, as shown in Figure 1.[56] Naturally occurring SODs contain metal centers like Ni, Fe, Mn, and Cu or Zn (NiSODs, FeSODs, MnSODs, and CuZnSODs, respectively). SODs catalyze the breakdown of superoxide radicals via the ping-pong mechanism, where superoxide acts alternatively to reduce the oxidized metal ion and then oxidize the reduced metal ion.[57] Nanoceria is the most widely studied nanozyme with SOD-like activity because of its capability to catalyze redox reactions, low toxicity, and high biocompatibility. The SOD-mimicking activity of cerium-based nanomaterials is attributed to the redox switching between Ce^{3+} and Ce^{4+}. The transformation generates a defect in the lattice structure by losing oxygen and electrons, which leads to the SOD-mimicking activity of this nanozyme.[58] Many other metal and metal oxide nanozymes also exhibit SOD-like activity such as those based on Au, Pt, Mo, Fe, Mn, Ni and some nitrides and sulfides.[59] Hydrophilic carbon clusters (HCCs) which were formed by the oxidation of single-walled carbon nanotubes with nitric acid and sulfuric acid were also reported to exhibit SOD-like activity.[60]

2.4. Catalase-Mimicking Nanozymes

Catalases are a family of antioxidant enzymes that are ubiquitous in all organisms exposed to oxygen, including plants, animals, and bacteria. Catalases catalyze the disproportionation of H_2O_2 into H_2O and O_2 (Figure 1).[61] H_2O_2 is a harmful by-product formed from several normal metabolic processes. Thus, catalases have an important role in protecting cells from oxidative damage caused by ROS. Nanozymes with catalase-like activities have been used as sensitizers for treating cancer using chemotherapy, photodynamic therapy, and radiotherapy.[62] Importantly, the catalase activity of nanozymes is highly sensitive to pH, temperature, and
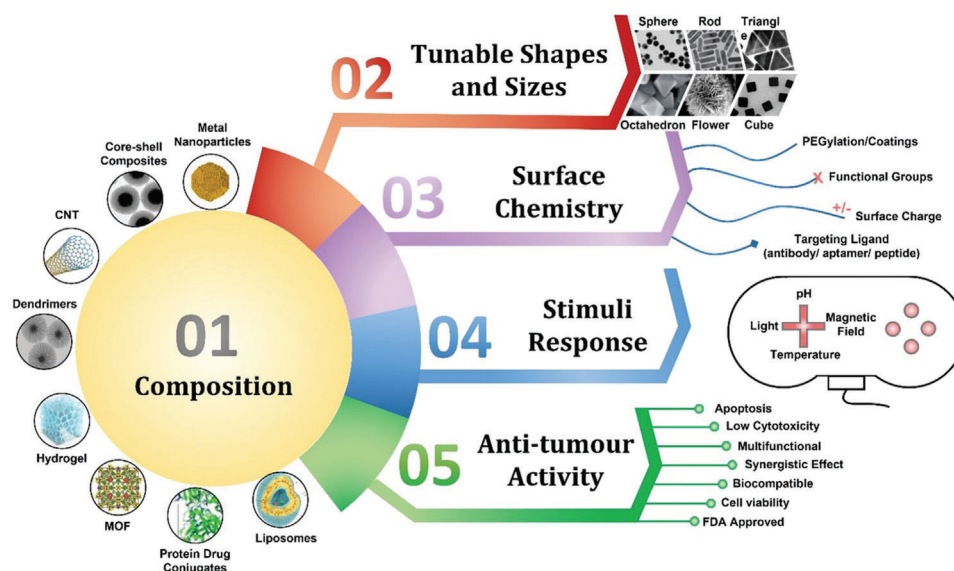
ADVANCED
SCIENCE NEWS
www.advancedsciencenews.com

ADVANCED
HEALTHCARE
MATERIALS
www.advhealthmat.de

Figure 2. Determination of nanozyme activity using standard chromogenic assays; A) TEM images of three typical peroxidase nanozymes based on Fe_3O_4, carbon, and gold; scale bars 200, 200, and 100 nm, respectively. B) All the three nanozymes exhibited peroxidase activity and induced oxidation of TMB, DAB, and OPD substrates clearly visible from the color change. C) Left, reaction time curves for the TMB oxidation reaction, center, the reaction time curves selectively shown from 0–60 s, right, comparison of the specific activities for the three nanozymes, determined using the nanozyme activity standardization method and D) comparison of the determined kinetic constants for Fe_3O_4, carbon, and gold nanozymes against horseradish peroxidase (HRP). Reproduced with permission.[177] Copyright 2018, Springer Nature.

TME. The onsite generation of O_2 by nanozymes has sparked wide interest because of its potential to alleviate hypoxia during tumor therapy.[22] The catalase-mimicking nanozyme, $SnFe_2O_4$, was successfully applied in multiple treatment modalities in vitro and in vivo, and achieved high photothermal conversion efficiency under irradiation with a 808 nm laser.[34] Wang et al. developed TiO_2 modified palladium nanosheets with inherent catalase-like activity for synergistic photodynamic and phototherapies.[28] A photo-enhanced synergistic catalytic mechanism of $PtFe@Fe_3O_4$ was reported with intrinsic peroxidase-like and catalase-like activities in the acidic TME and was observed to kill tumor cells by incapacitating tumor hypoxia.[16a] Li and colleagues developed a nanozyme, Fmoc-Cys/Fe@Pc/ACF, which actively released Fe^{3+} ions and zinc(II) phthalocyanine-based photosensitizer (ZnPc) in the tumor microenvironment. The released Fe^{3+} was responsible for the catalase-like activity,

**ADVANCED
SCIENCE NEWS**

www.advancedsciencenews.com

**ADVANCED
HEALTHCARE
MATERIALS**

www.advhealthmat.de

Figure 3. Schematic representation of characteristics of nanozymes and its applicability for treating cancer. Reproduced under the terms of the CC-BY license.[188] Copyright 2019, the Authors. Published by Springer Nature; Reproduced with permission.[189] Copyright 2019, Elsevier; Reproduced with permission.[190] Copyright 2020, Springer Nature; Reproduced with permission.[191] Copyright 2014, Wiley-VCH GmbH; Reproduced with permission.[192] Copyright 2021, Wiley-VCH GmbH; Reproduced with permission.[84] Copyright 2021, the Royal Society of Chemistry; Reproduced under the terms of the CC-BY license.[193] Copyright 2014, the Authors. Published by MDPI; Reproduced under the terms of the CC-BY license.[194] Copyright 2021, the Authors. Published by Springer Nature; Reproduced under the terms of the CC-BY license.[195] Copyright 2022, the Authors. Published by Wiley-VCH GmbH; Reproduced with permission.[196] Copyright 2012, Wiley-VCH GmbH; Reproduced under the terms of the CC-BY license.[197] Copyright 2018, the Authors. Published by American Chemical Society; Reproduced under the terms of the CC-BY license.[198] Copyright 2017, the Authors. Published by the Royal Society of Chemistry; Reproduced with permission.[199] Copyright 2012, The Royal Society of Chemistry; Reproduced with permission.[200] Copyright 2010, Wiley-VCH GmbH.

and it also promoted the photosensitizing activity of the released ZnPc enhancing the effects of photodynamic therapy.[63] The Pt-Ce6 nanozyme with catalase-like activity improved the photodynamic effect when compared to free Ce6 treated cells by decreasing the mitochondrial membrane potential, resulting in apoptosis.[64] From the above examples, it is evident that different catalase-mimicking nanozymes can be effectively used in cancer therapy.

3. Design and Synthesis of Nanozymes for Cancer Diagnosis and Therapy

The research on the development of nanozymes has significantly expanded since the inception of the first nanozyme (i.e., Fe_3O_4) in 2007.[65] The rapid adoption of nanozymes for cancer treatment necessitates the strategic design and development of nanozymes with robust catalytic activity, multifunctionality, tunable activity, and high stability. The enzymatic activity of nanozymes can be regulated through the control of their composition, morphology, and surface properties.[66] Today, many synthetic techniques are available for preparing nanomaterials in different shapes and sizes. Multifunctional nanozymes are typically multicomponent nanocomposites where other materials are incorporated to achieve specific functionalities. Heavy metals with high atomic number (Z) are used as radio sensitizers for radiotherapy. Similarly, conductive metals like copper, silver, gold, and platinum are ideal for photothermal and photodynamic therapy because these metals support plasmon excita-

tion by light irradiation, exhibit tuneable plasmonic response and are also known to be biocompatible.[67] **Figure 3** depicts the important characteristics of nanozymes. The composition can be considered a primary characteristic because it governs the basic framework upon which other tumor remediation functionalities are added. The different types of nanozymes can be broadly classified into eight types based on composition as metal, alloy, and metal oxide nanoparticles, core–shell composites, different carbon allotrope-based nanozymes such as nanozymes based on carbon nanotubes, graphene, nanodiamonds, carbon quantum dots, dendrimers, hydrogels, ordered porous materials like metal-organic frameworks (MOFs), protein–drug conjugates and liposomes. This section describes some well-understood nanomaterials and their functions which underpin the importance of rational design and synthesis of nanozymes.

Nanoceria-based nanozymes have been widely explored for their potential to be used in cancer therapy due to their redox activity and biocompatibility. Murugan et al. reported nanoceria-decorated, flower-like MoS_2 nanoflakes with intriguing multifunctional activities. In the TME, the nanozyme exhibited catalase-like activity and induced oxidative stress through the generation of ROS, which resulted in cancer cell apoptosis. In contrast, the same nanozyme scavenged free radicals in normal cells and protected them against oxidative damage.[68] In another study, ceria nanorods were identified to trigger apoptosis by reducing the mitochondrial membrane potential and inducing ROS production.[69] A dual lock and key type nanotherapeutic platform was also developed using ceria

2300768 (6 of 28)

ADVANCED
SCIENCE NEWS

www.advancedsciencenews.com

ADVANCED
HEALTHCARE
MATERIALS

www.advhealthmat.de

nanotubes which displayed cytotoxicity against HeLa cells and selectivity toward tumor tissues after intratumoral injection.[70]

Apart from nanoceria, metal nanoparticle-based nanozymes such as gold-, silver-, copper-, palladium-, and platinum-based nanomaterials have received considerable interest for use as effective cancer therapeutic agents.[71] Interestingly, many metal nanoparticles show pH responsive enzymatic activities. At a lower pH, they exhibit peroxidase-like activity and at higher pH they mimic catalase activity.[71] For example, both silver and gold nanoparticles exhibit enzyme-mimicking properties that have been investigated for treating cancer. Chong et al. observed that Au–Ag@HA nanoparticles displayed effective tumor therapeutic outcomes by boosting the production of •OH radicals and the release of toxic Ag^+ ions in the tumor sites.[72] Gold nanoparticles can penetrate cell membranes and cellular compartments to induce necrosis by generating oxidative stress.[73] Similarly, copper-based nanozymes have also exhibited enzyme-mimicking activity that can be used in advanced cancer therapies.[74] A hollow PtCo nanosphere based radiosensitizer nanozyme was identified to augment the generation of ROS and induce cell apoptosis upon X-ray irradiation while at the same time demonstrating efficient radiosensitization capability of PtCo.[75] A composite nanozyme, AuPtAg-GOx, has been reported for synergistic tumor immunotherapy due to its catalase activity and glucose consumption in the presence of O_2 resulting in effective starvation therapy.[76] Mesoporous carbon-gold hybrid nanozymes were used for real-time imaging of tumor and photothermal therapy.[77] Gold nanoparticles embedded in hollow carbon shell nanospheres induced ROS generation when irradiated with an 808 nm-laser.[78]

Metal oxide nanoparticles have been explored as nanozymes for cancer therapy. Metal oxide-based nanozymes usually act by inducing ROS generation, which can help overcome some types of cancer cell drug resistance, as well as perform selectively in the tumor microenvironment. Fe_3O_4-based nanozymes have been abundantly studied for tumor remediation owing to their enzymatic activity.[79] For example, the catalytic activity of Fe_3O_4@C nanoparticles modified with folic acid was enhanced by adding ascorbic acid, and the composite nanozyme triggered oxidative stress in cancer cells without destroying normal cells.[80] Surface and bulk modification of Fe_3O_4 nanoparticles allow for incorporating additional functionalities and synergistic coupling with other treatments to increase the therapeutic efficacy.[37,81] For instance, PtFe@Fe_3O_4 nanozymes exhibited intrinsic photothermal activity and photo-enhanced peroxidase- and catalase-like properties in the acidic TME and effectively induced cell death in tumor cells by relieving tumor hypoxia.[16a] Wang et al. developed cobalt-doped Fe_3O_4 nanozymes possessing higher peroxidase activity that could induce a ROS burst to kill renal cancer cells.[82] Hepatocellular carcinoma (HCC)-targeted HccFn(Co_3O_4) was observed to be a promising nanozyme for HCC tumor prognostic diagnosis due to its specific targeting ability.[83]

Ordered porous materials, which are also called porous crystalline frameworks[84] and include zeolites, metal-organic frameworks (MOFs), covalent organic frameworks (COFs), and covalent triazine frameworks (CTFs), are an emerging class of nanomaterials that are being increasingly investigated for use in cancer therapy. These materials exhibit some unique properties which are highly useful for therapeutic modalities, such as high surface area and tuneable surface characteristics which allow uniform dispersion and loading of active antitumor agents and stimulus-responsive characteristics. Prussian blue, a synthetic blue pigment, is a MOF that is approved by the FDA for its use in clinical magnetic resonance imaging.[85] Prussian blue nanoparticles were effective for cancer diagnosis and treatment in vitro and in vivo due to their good catalytic activity in scavenging ROS.[86] Platinum-doped Prussian blue (PtPB) nanozymes were identified to enhance photothermal efficiency and paved the way for the application of multimodal imaging whilst preserving good biosafety levels.[87] Hollow Prussian blue nanoparticles containing Au-Pt nanozymes loaded with Ce6 reduced lung metastases by overcoming hypoxia and enhanced the effectiveness of PDT.[88] Other relatively recent studies reported that the loading of platinum nanoparticles on photosensitizing MOFs resulted in enhanced efficiency for photodynamic therapy.[26]

The composition of the nanosystems can be further regulated by doping or the incorporation of functional molecules that can enhance the treatment efficacy. Doping of metal-oxide nanomaterials with metal ions is a commonly used strategy to control the enzymatic activities of nanozymes. The doping of metal ions onto metal-oxide nanomaterials creates surface defects and regulates the oxidation states of surface metal ions. For instance, doping of cobalt onto a Fe_3O_4 nanozyme augmented its peroxidase activity and catalyzed the decomposition of H_2O_2 at very low doses of Co@Fe_3O_4 nanozyme, thereby destroying human renal tumor cells both in vitro and in vivo by ROS bursts.[82] Though a plethora of nanozymes can be used to enhance the treatment efficacy, tuning them for desired functionality is essential for developing effective therapies for alleviating cancer with minimal side effects. Among the various physical properties of nanozymes, their morphology plays an important role in governing their enzymatic activities. This is due to the relative fraction of different crystal planes which are exposed, the length of pores oriented in specific crystallographic directions in ordered porous materials, as well as the specific surface area, target recognition and binding being all dependent on morphology. Thus, morphology can significantly impact the catalytic activity of nanozymes in cancer treatment. Recent literature has seen the use of a variety of nanozymes with different morphologies, such as nanospheres, nanoflowers, nanosheets, nanorods, nanowires, nanoflakes, and nanocubes.[89] Many reports concluded that modulation of the shape and morphology of nanozymes directly control their inherent catalytic activities.[90] For instance, Liu and other researchers revealed that the peroxidase activity displayed by Fe_3O_4 nanocrystals was different for spheres, octahedral, and triangular plates because the peroxidase activity relied on the differential exposure of Fe_3O_4 nanocrystal facets.[91] Similarly, particle size also regulates nanozyme activities. For instance, the photothermal conversion efficiencies of gold nanoparticles increased when the size of the particles was decreased, indicating a direct correlation between their size and enzymatic activities.[92]

In addition to the composition, size, shape, and morphology of the nanozymes, their surface characteristics also influence their enzymatic properties and their specificity because the surface is usually actively involved in the catalytic reactions and recognition and binding events occur primarily on the surface of the nanozymes. Thus, the optimization of surface properties is essential for obtaining the desired enzymatic activities, site

**ADVANCED
SCIENCE NEWS**

www.advancedsciencenews.com

**ADVANCED
HEALTHCARE
MATERIALS**

www.advhealthmat.de

specificity and adequate biocompatibility.[93] For instance, a 20-fold increase in the catalytic efficiency of Fe_3O_4 nanozymes was observed when a histidine residue was introduced into the nanosystem to mimic the enzymatic activity of natural horse radish peroxidases.[94] Studies conducted by Zhou et al. also concluded that the surface modification of the nanozymes influenced their selectivity. For instance, an enantioselective nanozyme consisting of gold nanoparticles (AuNPs), chiral cysteine (Cys) and expanded mesoporous silica (EMSN) (D-Cys@AuNPs-EMSN) exhibited selective binding to L-DOPA whereas L-Cys@AuNPs-EMSN exhibited selectivity towards D-DOPA because of the chiral selectivity during the formation of hydrogen bonds between chiral Cys-and DOPA.[66]

In addition to the above-discussed factors, the behavior of nanozymes in biological media must be considered because the protein corona formation may have a significant effect on the catalytic activity of the nanozymes.[93,95] Thus, understanding the physicochemical properties of nanozymes is key to guiding their rational design for cancer therapeutic applications.

4. The Tumor Microenvironment

The term "tumor microenvironment" refers to the heterogeneous biological environment around a tumor, which includes specific innate and adaptive immune cells, exosomes, fibroblasts, extracellular matrix, stroma, signaling molecules, and blood vessels.[96] It is also associated with unique biochemical and metabolic characteristics, such as altered redox levels, lower pH and oxygen levels or higher temperature than the surrounding somatic tissue. The tumor and the TME can be visualized as a single living entity because they constantly interact with and influence each other. The tumor can influence the TME by releasing extracellular signals to control peripheral immune tolerance and promote tumor angiogenesis. Similarly, the immune cells in the TME can influence the growth and tolerance of tumor cells. The TME also employs the complex signaling networks that are used by normal cells. Thus, the tumor cells grow by recruiting the energy metabolism of normal cells through the bidirectional interactions between tumor cells and the TME. In the host tissue, tumor cells can also stimulate molecular, cellular, and physical changes to support their progression. The characteristics of cancer at a specific stage have been suggested to be demarcated by specific profiles reflecting their patterns of angiogenesis, resistance, proliferation, metastasis, hypoxic and acidic conditions, overexpression of glutathione, and an abnormal metabolic state.[97] This section briefly discusses the TME with the prospect of exploiting it for effective cancer therapy.

4.1. Hypoxia

Hypoxia refers to the condition where insufficient oxygen is available in the tissue to maintain adequate homeostasis. It is commonly observed in solid tumors because rapidly dividing tumor cells consume the accessible oxygen leading to the hypoxic condition. Hypoxia is understood to be a consequence of the inconsistent red blood cell flux in the abnormal tumor vasculature.[98] Typically, the oxygen concentration in normal tissues is in the

range of 3–6%, whereas the oxygen concentration can be depleted to the range of 1–2% in hypoxic solid tumors.[99] Hypoxia contributes to tumor progression and tumor cell resistance by promoting abnormal angiogenesis (formation of the new blood vessels), desmoplasia (growth of fibrous or connective tissue), and inflammation.[100] In the case of chronic hypoxia or diffusion-limited hypoxia, tumor cells within a 180 μm periphery of blood vessels are in danger of necrosis (death of cell or tissue) due to spatial distortion of tumor vasculatures leading to an increase in inter-capillary distance. The variable blood flow or temporary blockage in tumor blood vessels can lead to other types of hypoxia, such as acute hypoxia, perfusion-limited hypoxia or intermittent hypoxia.[101] In tumor tissues, hypoxia was observed to suppress the immune response. Correspondingly, hypoxia results in resistance to tumor therapy through various mechanisms. Hypoxia-inducible factor-1 (HIF-1), which consists of HIF-1α and HIF-1β, is responsible for mediating hypoxia-induced signaling and is a regulator of O_2 homeostasis. HIF-1-induced genes regulate various cellular functions, including cell growth, angiogenesis, survival, motility, and cell differentiation. The increased HIF-1 activity promotes tumor development.[102] Besides, the tumor stromal microenvironment also changes due to hypoxia leading to a reduced number of stromal cells (cells that build the connective tissue in a tumor) and loss of normal tissue structure that affects the stromal structure.[103]

Evidence also suggests that hypoxia overpowers immune response and endorses metastasis.[98] Clinical studies have proven that patients with hypoxic tumors have significantly lower survival rates as the low concentration of oxygen-free radicals cannot generate enough ROS via radiotherapy to cause cell death in these tumors.[104] Hypoxia also induces variations in gene expression, which ensues proteomic changes that impact several cellular and physiological functions and restrain patient prognosis. The resistance to therapy by hypoxia is caused by slow proliferating stem-cell-like cell phenotypes, decreased senescence, malfunctioning of blood vessels, and metastasis.[105] Hypoxia-induced epithelial-to-mesenchymal transition (EMT) increases the aggressiveness and metastatic potential of tumor cells, wherein the tumor cells undergo EMT by reducing intercellular attachments, cell–cell contacts, and enhanced motility. The efficacy of conventional treatments is unsatisfactory due to the hypoxic tumor microenvironment. Thus, effective cancer therapies require dedicated functionalities to overcome the challenges presented by hypoxia. Several nanozymes have demonstrated high catalase-like activity to catalyze the disproportionation of H_2O_2 to yield O_2 (and O^{2-}) for easing tumor hypoxia and enhancing PDT or RT.[106] Efforts are being made to develop TME responsive nanozyme-based catalytic therapy.[107]

4.2. Tumor Acidity

Increased acidity is a characteristic feature of hypoxic tumor and their microenvironment. Generally, normal cells produce lactic acid exclusively during oxygen deprivation and gain energy through aerobic respiration and lactic acid fermentation. Aerobic respiration occurs in the presence of oxygen and comprises glycolysis, Krebs' cycle, and oxidative phosphorylation, whereas, in lactic acid fermentation, glucose is converted into pyruvate

and later reduced to lactate in the absence of oxygen. Tumor cells derive adenosine triphosphate (ATP) from glucose as the primary source of carbon through glycolysis following the Warburg hypothesis.[108] According to the Warburg effect, glucose gets converted to lactic acid via the glycolytic pathway, which leads to dramatic increase in glucose consumption and higher production of H^+ ions. The anaerobic glycolysis pathway yields only two ATP molecules, whereas aerobic respiration yields 36 ATP per molecule of oxygen. Thus, in tumor cells, the downstream glycolytic enzymes will be overexpressed to meet the demand for energy caused by rapidly dividing tumor cells. In malignant tumors, an acidic extracellular pH of 6.5–6.9 (compared to physiological pH values of 7.2–7.4), is often observed due to the excretion of H^+ ions because of poor tumor vascular perfusion. The efflux of H^+ ions exposes adjoining non-cancerous cells and can lead to their death.[109] The high conversion rate of pyruvate to lactate can also be due to the overexpression of lactate dehydrogenase A, which adds to the tumor acidity.[110] Moreover, carbonic anhydrase (CA) also contributes to the production of H^+ and HCO_3^- by hydrolyzing CO_2 produced during the pentose phosphate pathway.[111] The tumor's acidic environment is detrimental to normal cells as it promotes the degradation of the extracellular matrix by proteinases, intensifies angiogenesis, and inhibits the immune response to tumor antigens. Interestingly, tumor cells can resist acid-induced cellular toxicity and maintain their growth even at decreased pH. Furthermore, tumor acidity is also due to the unusual tumor vasculature that is leaky, poorly organized, and disrupts blood flow and oxygen supply.[109] The acidic pH in tumor cells can be utilized to design stimulus-responsive systems by inducing the release and increasing the accumulation of drugs in the tumor with reduced leakage into normal tissues. Furthermore, intelligent engineering of smart nanomaterials which target the reduced peritumoral pH may offer an alternative more targeted approach compared to traditional therapies.

4.3. Reactive Oxygen Species

Reactive oxygen species (ROS) are the by-products of cell metabolism and include reactive ions and molecules like hydroxyl radicals (•OH), singlet oxygen ($^1O_2$) and superoxide radicals ($O_2•^-$). Generally, intracellular ROS will serve as envoys in many signaling pathways.[112] Several biochemical reactions maintain an equilibrium between the generation and elimination of ROS,[113] but increased ROS levels can promote tumor growth and induce the probability of DNA mutations, which can increase tumor resistance to elimination by the natural immune mechanisms or by external therapies, or conversely, can also trigger apoptosis.[114] The elevated ROS levels create an imbalance between the oxidative stress and the antioxidant defense mechanisms, which leads to genomic instability, mutation, and damage to DNA repair pathways. Higher levels of ROS also damage proteins, DNA and RNA, leading to mutations that can promote cancer in normal cells and impart multi-drug resistance to cancer cells. Cancer stem cells are also impacted by ROS levels through blockage of self-renewal capabilities or differentiation stimulation leading to tumor heterogeneity.[115] The inflection in the transcription factors results in the accretion of ROS, leading to cellular transformations of human mesenchymal stem cells (hMSCs). Apoptosis in cancer cells is also mediated by the levels of ROS and leads to cancer cell resistance by activation of redox-sensitive transcription factors such as NF-κB, nuclear factor (erythroid-derived 2)-like factor 2 (Nrf2), c-Jun, and HIF-1α. Thus, the regulation of ROS is indispensable for the cellular process and understanding the multifaceted connection between ROS levels, and cancer is necessary for the development of effective cancer treatment modalities. For instance, interference in ROS homeostasis through cascade-amplified ROS generation and the waning of antioxidant defense has been recognized as effective strategy for anti-cancer therapy.[114] The use of nanozymes has shown tremendous potential in anti-cancer therapies, and many studies have focused on understanding the role of ROS in tumor promotion or suppression.[8a] Notably, good evidence has been presented supporting both ROS as a tumor promoter and a tumor suppressor. Thus, substantiating a better understanding of the impact of ROS, specific to a particular applied therapy, will be critical for improving such cancer treatments. Nanozyme-based cancer therapeutics have sparked wide interest for their ability to regulate cellular ROS levels for cancer therapy.[116]

From the above discussion, it is evident that a good understanding of the TME is a prerequisite for the development of effective chemotherapeutics and that the TME can be strategically exploited to achieve tumor specificity, improve the therapeutic index, and pharmacokinetic profile of chemotherapeutics. The high enzymatic activities, specificity, biological stability, and tunability of nanozymes make them ideal therapeutic agents for the alleviation of the problems with traditional cancer treatments and the development of effective cancer chemotherapeutics.

5. Nanozymes for Cancer Diagnosis

The success rate of treatment, recovery, and patient survival can be significantly increased by the early diagnosis of cancer. Early and accurate detection of cancer can be effective in improving patient's condition. Since cancer is associated with changes in genes and many specific receptors are overexpressed on cancer cells, the use of nanozymes to specifically detect these changes and receptors has gained much attention. The ensuing section briefly highlights the use of nanozymes for cancer diagnosis.

5.1. Nanozymes for Cancer Diagnosis in Liquid Biopsies

The liquid biopsy diagnosis of cancer refers to the detection of hallmarks of cancer or cancerous cells in bodily fluids. The in vitro diagnosis techniques need to be fast, scalable, and autonomous for the practical and accurate identification of tumor onset, continuous monitoring, and to support preventive healthcare. This diagnosis can be performed by detection of specific cancer-associated circulating proteins such as CA-125 (ovarian cancer), PSA1 (prostate cancer), human epidermal growth factor receptor 2 (HER2) (subtypes of breast cancer and other cancers), carcinoembryonic antigen (colon cancer), or other proteins, DNA and RNA molecules associated with tumors.[12,117] Emerging literature also suggests the addition of immune cell-derived markers, such as inflammatory cytokines is able to enhance diagnostic accuracy.[118]

**ADVANCED
SCIENCE NEWS**

www.advancedsciencenews.com

**ADVANCED
HEALTHCARE
MATERIALS**

www.advhealthmat.de

A direct approach for in vitro diagnosis of cancer is the detection of circulating tumor cells (CTC) in body fluids. Circulating tumor cells can lead to the development of primary tumors and metastatic lesions. In CTC sensors, the design of the receptor component is critical for accurate detection. Appropriate binding molecules must be grafted on the surface of the receptor material for it to recognize and selectively bind to the targeted cancer cells. Different strategies for the functionalization of sensor receptor material to enable selective binding with cancer cells have been reviewed previously.[119] The transduction of CTC information into useful electrical signals can be done using a variety of platforms such as electrochemistry, optical spectroscopy, surface plasmon resonance, surface-enhanced Raman scattering, gravimetry, fluorescence, cell-affinity micro-chromatography, chromogenic assays, label-based or label-free immunoassays, antibody-based assays, single-cell secretion assays, physical sorting in microchannels, and dielectrophoresis.[118,119d,120]

Nanozymes can be employed for CTC diagnosis using surface functionalization techniques for selective binding to cancer cells and detection using a suitable transduction platform. Commonly, nanozymes are coupled with chromogenic substrates to enable easy and fast optical readout in laboratory settings. For instance, Maji et al. observed unprecedented theranostic activity for composite nanoparticles consisting of mesoporous silica, graphene oxide, and folic acid when decorated with Au nanoparticles. The nanozyme system allowed the diagnosis of cancerous HeLa cells through the oxidation of the chromogenic substrate TMB in the presence of H_2O_2 and an associated color change.[121] In addition, the developed nanozyme was also active for catalytic cancer therapy since it generated reactive oxygen species (ROS, •OH) that damaged the cancer cells in the presence of both endogenous and exogenous H_2O_2. The developed nanozyme was also selective toward cancerous HeLa cells and exhibited no obvious damage or detection of normal human embryonic kidney HEK 293 cells.[121]

Ferritin is a natural cage-like protein that has been explored for the design of nanozyme systems owing to its self-assembly capabilities and spherical structure. Fan et al. pioneered the use of nanozymes encapsulated in ferritin for the direct detection of cancer cells using chromogenic substrates.[122] Peroxidase mimicking iron oxide nanoparticles were encapsulated inside a recombinant human heavy-chain ferritin (HFn) protein shell, which is selectively bound to transferrin receptor 1 (TfR1) overexpressed by tumor cells. The developed magneto protein nanozyme allowed the colorimetric detection of nine different types of cancers with a sensitivity of 98% and specificity of 95%.[122] Following the same approach, Jiang et al. developed a ferritin-based cobalt oxide nanozyme for the selective detection of hepatocellular carcinoma (HCC).[83] HCC tissues are known to exhibit specific binding with SP94 peptide. The cobalt oxide nanoparticles were biomineralized inside the ferritin cage, and the SP94 peptide was genetically engineered on the external surface of ferritin for recognition of HCC cells. The developed ferritin-based nanozyme exhibited excellent peroxidase activity and allowed selective colorimetric detection of HCC cells with a sensitivity of 63.5% and specificity of 79.1%.[83]

Glutathione (GSH) is an important antioxidant that is found in all cells. GSH can be used as a biomarker for cancer cell detection because its concentration can be up to twofold higher in cancerous cells compared to non-cancerous cells.[123] Liu et al. demonstrated it is possible to detect GSH using a light-responsive nanozyme which could be switched between on and off states using visible light.[124] The developed nanozyme consisted of a custom-designed photosensitized metal-organic framework (PSMOF) which exhibited peroxidase-like activity for chromogenic substrates. The MOF was synthesized using a light-absorbing Ru(bpy)$_3^{2+}$ complex, H_2BPDC (4,4-biphenyldicarboxylic acid) ligand and zinc cations. The Ru^{II} complex was selected because of its strong absorbance in the visible region, which also imparted high peroxidase activity to the nanozyme under visible light.[124] Pang et al. successfully detected GSH using the growth dynamics of gold, viral biomineralized clusters (AuVCs).[125] In the absence of GSH, AuVCs exhibited a unique optical response and peroxidase activity for TMB oxidation in the presence of H_2O_2. However, in the presence of GSH, the biomineralization of the gold nanoparticles was affected, and lower peroxidase activity was observed with a shift in optical response. Thus, GSH concentration could be correlated with the optical response for the affirmation of cancer.[125] The above studies provide good evidence for the affirmation of cancer based on GSH levels. However, it is crucial to consider the sensitivity of the assays used for GSH detection to eliminate the possibility of false positives owing to the small difference between GSH levels of healthy and cancerous cells (differ by a factor of up to 2). The probability of a false positive is significantly lower when the difference between the concentration of a biomarker between healthy and cancerous cells is larger than an order of magnitude.

A cancer diagnosis can also be performed by the detection of DNA molecules associated with tumor cells. The detection of DNA molecules has conventionally depended on the polymerase chain reaction (PCR) or labeling of DNA prior to the assay. However, such assays are time-consuming. Single-stranded DNA molecules (ss-DNA) have recently emerged as effective probes for accurate recognition and selective binding to complementary DNA strands. Wang and colleagues demonstrated an interesting gated-nanozyme system for label-free detection of DNA molecules using the colorimetric reaction of TMB in the presence of H_2O_2.[126] The nanozyme consisted of peroxidase-mimicking platinum nanoparticles encapsulated inside mesoporous silica nanoparticles (Pt@mSiO$_2$). The Pt@mSiO$_2$ nanoparticles were subsequently functionalized with ss-DNA to obtain the closed-gate configuration of the nanozyme wherein ss-DNA molecules blocked the pore openings and prevented the oxidation of TMB by Pt nanoparticles present inside mSiO$_2$ nanoparticles. However, the ss-DNA molecules were removed from the surface of Pt@mSiO$_2$ nanoparticles when the Pt@mSiO$_2$-ss-DNA assembly was exposed to complementary DNA molecules. The exposure brought the nanozyme system to the open-gate configuration where Pt nanoparticles could access TMB molecules, oxidize them and induce color change.[126] Similarly, Bhattacharjee et al. demonstrated the detection of methylated DNA in colorectal cancer cell lines using peroxidase-mimicking mesoporous iron oxide (MIO) nanozymes and ss-DNA.[127] The target DNA was first extracted and denatured to obtain the ss-DNA which was applied to a bare screen-printed gold electrode. MIO nanozymes were then functionalized with a 5-methylcytosine antibody (5mC) which can recognize and bind methylated ss-DNA obtained from

colorectal cancer cell lines. The peroxidase activity of MIO-5mC composites allowed the detection of methylated DNA using the colorimetric reaction of TMB in the presence of H_2O_2. In addition, the binding event could also be followed electrochemically using a screen-printed gold electrode.[127]

The enzyme-linked immunosorbent assay (ELISA) technique has been extensively proven to have high substrate specificity, reliable biorecognition and enzyme-induced signaling. However, the low activity of some enzymes limits the wide-spread application of the ELISA technique. Thus, there are efforts to increase the efficacy of this technique by developing high activity nanozyme systems. For instance, Kim et al. employed the peroxidase activity of Fe_3O_4, and Pt nanoparticles encapsulated in mesoporous carbon to develop an ELISA assay for the detection of the cancer biomarker HER2 and diarrhea-causing rotavirus.[128] The developed nanozymes were conjugated with targeted cancer and virus receptors using complementary antibodies and exhibited 50 times higher activity than nascent Fe_3O_4 nanoparticles. The high peroxidase activity allowed fast detection of the target analytes in less than 3 min using the colorimetric reaction of TMB in the presence of H_2O_2.[128] Huang et al. demonstrated the detection of carcinoembryonic antigen (CEA) using catalytic cascades driven by hybrid nanozymes, that is, composites consisting of nanomaterials as well as natural enzymes.[129] In this study, to improve the activity of the enzyme horseradish peroxidase (HRP), it was encapsulated in PdCu hydrogels which consisted of complex 3D networks of 1D wires. The high surface area of the 3D network and favorable chemical interactions between the noble metals and HRP improved its stability and peroxidase activity. Similarly, glucose oxidase (GOx) was encapsulated in the MOF ZIF-8 to enhance its activity and stability. Functionalization of ZIF-8-GOx with CEA-specific antibodies allowed it to be used for a sandwich ELISA assay along with HRP-PdCu composite nanozymes to detect CEA.[129]

5.2. Nanozymes for In vivo Cancer Diagnosis

In vivo diagnosis of cancer refers to the detection of cancer inside a living organism, usually enabled or enhanced by the injection of suitable chemical/imaging agents. In vivo cancer diagnosis is performed using molecular labeling and imaging techniques such as fluorescence, ultrasound, magnetic resonance, photoacoustic, photothermal, and computed tomography imaging. ROS such as superoxide, hydroxyl radicals, and hydrogen peroxide are related to numerous ailments in the human body, such as cancer, diabetes mellitus, ischemia injury, and inflammatory and neurodegenerative diseases.[130] The overproduction of ROS can damage cellular lipids, proteins, and DNA, disrupting healthy body function. H_2O_2 has been considered a potential diagnostic biomarker for several ailments, including cancer, owing to its relatively long half-life and free diffusion in the human body.[130,131] The detection of H_2O_2 in vivo has been demonstrated using fluorescent probes, and ultrasonic and magnetic resonance imaging techniques. For instance, Yang et al. used Prussian blue nanoparticles (PBNPs) as a catalase-mimicking nanozyme for dual detection of H_2O_2 in the body using ultrasonic and magnetic resonance imaging.[132] Ultrasound imaging has conventionally depended on using ultrasound contrast agents such as pre-formed gas microbubbles. However, these microbubbles are unstable and decompose rapidly after injection in the human body. In contrast, catalase mimicking PBNPs converts endogenous H_2O_2 into O_2, leading to the in situ generation of gas microbubbles. Thus, PBNPs can be used as smart ultrasound contrast agents, which generate contrast only at malignant sites where H_2O_2 is overexpressed. In addition, the PBNPs attain a unique structure in water where water molecules coordinate with the paramagnetic Fe^{III} centers leading to modification of their magnetic properties. This results in the enhancement of contrast in magnetic resonance imaging due to the shortening of T_1 relaxation time driven by paramagnetic PBNPs and in situ generated paramagnetic oxygen microbubbles. Thus, PBNP nanozymes allowed a dual-mode detection of H_2O_2.[132] Gong et al. demonstrated the use of oxygen-deficient $FeWO_x$ nanosheets as ratiometric probes for photoacoustic imaging of endogenous H_2O_2 and multimodal imaging based on magnetic resonance and computed tomography imaging.[133] $FeWO_x$ nanosheets exhibited peroxidase-mimicking activity for the decomposition of H_2O_2 into hydroxyl radicals. The ratiometric probe was obtained by co-loading of 3,3,5,5-tetramethylbenzidine (TMB) and IR780 dye on the $FeWO_x$ nanozymes, which allowed ratiometric photoacoustic imaging in subcutaneous 4T1 (breast cancer cell line) xenograft tumor and lipopolysaccharide (LPS)-induced inflammation models. The high contrast in magnetic resonance was obtained from the presence of iron, and in computed tomography imaging due to the presence of heavy metal tungsten, in the combined synthesized nanozyme.[133] Feng et al. elaborated on the use of PEG-functionalized ultrasmall tin ferrite ($SnFe_2O_4$, SFO) nanoparticles as nanozymes for enhanced photothermal and photo-chemodynamic therapy.[34] The SFO nanoparticles had an average diameter of 9.3 nm and exhibited peroxidase, catalase, and glutathione peroxidase activity. The generation of hydroxyl radicals facilitated chemodynamic therapy, whereas the catalase activity of the SFO nanozyme relieved tumor hypoxia, and the glutathione peroxidase activity depleted the glutathione level of tumor cells to increase the efficacy of the chemodynamic therapy. Moreover, the synthesized nanozyme exhibited a high photothermal efficiency of 42.3% as well as photothermal modulation of the therapeutic activity. The presence of tin and iron in the nanozyme also allowed magnetic resonance and computed tomography imaging and, thereby, online monitoring of the photo-chemodynamic therapy.[34] Wang et al. suggested the use of $Ag_2S@Fe_2C$ quantum dots as visualization nanozymes for multimodal imaging and intensive combination therapy for breast cancer.[134] The nanozymes exhibited peroxidase-mimicking and photothermal activity with low off-target toxicity. Up to 90% of the nanozyme injected during the treatment of in vivo mouse models was reported to be excreted from the body within 14 days. Moreover, the photothermal activity of the nanozyme resulted in a remarkable performance in near-infrared and magnetic resonance imaging.[134]

Due to interference from the biological matrix, ratiometric imaging methods, which employ internal standards, are more accurate and sensitive than single-output imaging methods. Near-infrared fluorescent imaging (NIRF) exhibits high sensitivity and rapid response, whereas photoacoustic (PA) imaging provides high imaging depth and spatial resolution. Teng et al. developed an oxidase-mimicking nanozyme (MSPN) consisting

of manganese oxide nanoparticles, an organic semiconductor (PFODBT) and an oxidase-responsive molecule (ORM) for combined near-infrared fluorescence and photoacoustic dual-mode imaging and cancer therapy.[53] The PA signal of PFODBT at 680 nm and the NIRF signal at 695 nm, along with the PA signal of ORM at 780 nm and the NIRF signal at 825 nm, served as internal references. In the TME, oxidase mimicking MnO_x nanoparticles generated superoxide radicals for tumor cell apoptosis. The oxidase activity also led to the decomposition of the oxidase-responsive molecule leading to a decrease in PA signal intensity at 780 nm. In contrast, the signal intensity at 680 nm due to PFODBT remained constant. Similarly, the decomposition of the ORM led to decreased emission at 825 nm and increased emission at 695 nm owing to effective fluorescence resonance energy transfer between PFODBT and ORM. Thus, the developed nanozyme exhibited remarkable in vivo theranostic activity through superoxide radical-mediated catalytic therapy and ratiometric NIRF-PA-based dual-mode cancer imaging and monitoring.[53]

Cao et al. reported an all-in-one $Fe_3O_4/Ag/Bi_2MoO_6$ (FAB) nanozyme with multiple enzyme-mimicking properties for catalytic cascade therapy and multimodal imaging.[40] The synthesized nanozyme exhibited peroxidase, catalase, superoxide dismutase, and glutathione oxidase activity, which resulted in effective chemodynamic, photothermal, and photodynamic therapies driven by reactive oxygen species generation, tumor hypoxia relief and glutathione depletion. Laser irradiation for 7 min per day resulted in an 80% reduction of tumor volume compared to control and irradiation twice per day resulted in complete elimination of the tumor within 16 days. Moreover, the therapeutic action could be modulated and monitored using photoacoustic, photothermal, and magnetic resonance imaging.[40] While cancer theranostics employing near-infrared I radiation (NIR-I, 650–1000 nm) have been widely investigated, the reports on the use of near-infrared II (NIR-II) imaging and therapy are increasing in the recent literature owing to associated benefits such as deeper tissue penetration, lower photon scattering, lower background interference, and maximum permissible exposure.[117]

6. Smart Nanozymes for Modulation of the TME and Synergistic Cancer Therapy

Nanotechnology can be a powerful tool to design therapeutics that can disrupt the TME balance. In this article, such nanozymes have been called smart nanozymes, which strategically exploit the TME by in situ generation of reactive species or modulate the TME itself to improve the effectiveness of the therapy. Many examples of such smart nanozymes have been discussed in the earlier sections. The hallmark of any solid tumor is its TME, containing tumor cells, immune cells, and somatic cells within, and environment characterized by acidosis and low levels of oxygen, coupled with elevated levels of reactive oxygen species. The TME can present a strong barrier to some conventional cancer treatments and can also be responsible for promoting tumor metastasis, recurrence, and resistance.[135] Thus, this section particularly focuses on two types of smart nanozyme that induce damage to or terminate the cancer cells by the generation of ROS or through hypoxia relief.

6.1. ROS-Generating Nanozymes for Cancer Therapy

When compared to normal cells, tumor cells are more susceptible to exogenous ROS. Thus, attempts have been made to develop ROS-mediated cancer therapy with high tumor specificity, therapeutic effect, and less toxic side effects.[93,136] FDA approved cancer therapies such as photodynamic therapy already exploit ROS generation induced by external stimuli to kill tumor cells. However, these present some limitations, such as relatively low concentration of generated H_2O_2 and low light penetration into tissues. ROS-generating nanozymes are strategically designed for ROS production without the need of an external stimulus. Different types of nanozymes with POD-like activity have been employed for monitoring glucose levels in human serum,[137] cancer detection,[89a] and have been studied for cancer therapy.[138] For example, the glucose oxidase conjugated with an iron oxide nanozyme with peroxidase-like activity was identified to catalyze a cascade of enzymatic reactions wherein glucose is converted to gluconic acid and H_2O_2 by glucose oxidase and H_2O_2 to hydroxyl radicals by peroxidase nanozymes.[139] Several nanozyme-based multi-enzyme systems have also attracted interest for their potential cancer theranostic applications.[65,139b,140]

Ever since the discovery of Fe-based nanoparticles possessing peroxidase-like behavior, several iron-based nanomaterials have been developed for tumor inhibition and cancer treatment.[40,141] A summary of various nanosystems that generate ROS and are usable for cancer treatment is presented in **Table 2**.[68,78,107,142–154] Wang and co-authors investigated peroxidase-mimicking nanozymes, for example, SiO_2, TiO_2, ZnO, Fe_2O_3, Fe_3O_4-10 nm, Fe_3O_4-25 nm, Fe_3O_4-50 nm, Fe_3O_4-150 nm, Ag, $Cu(OH)_2$, and V_2O_5, and identified that POD-like nanozymes induced a novel form of cell death, termed nanoptosis, which was morphologically and biochemically distinct from other well-defined forms of cell death such as apoptosis, necrosis, autophagy, pyroptosis, and ferroptosis.[141] The POD-like activity of investigated nanozymes was dependent on their physicochemical properties, such as metal ions on the surface of iron oxide nanoparticles, particle sizes, and surface modifications. Nanoptosis induced by Fe_3O_4-10 nm nanozyme was compared with a control sample consisting of HePG2 cells treated with phosphate-buffered saline (PBS), apoptosis induced by staurosporine, necrosis induced by H_2O_2, autophagy induced by rapamycin, pyroptosis induced by nigericin, and lipopolysaccharide and ferroptosis induced by erastin.[141] **Figure 4** depicts the morphological and biological changes induced in HepG2 cells after exposure to Fe_3O_4-10 nm nanozymes for different durations and the comparison of cell death characteristics with the control. The authors concluded that apoptosis displayed unique morphological features of swelling and vacuolation of the mitochondria, disruption of the endoplasmic reticulum, chromatin condensation and margination, and disintegration of the nucleolus. Protein profile and gene expression of HepG2 cells using quantitative proteomics and RNA sequencing studies were conducted. When compared to the untreated control group, which was related to the ATP-citrate lyase (ACLY)-dependent rat sarcoma viral oncogene (RAS) signaling mechanism, 13 proteins were up- or down-regulated in the Fe_3O_4 nanozyme-treated group. As a result, the tumor volume in Fe_3O_4 nanozyme-treated mice was considerably reduced when compared to the control group, indicating a

Table 2. A summary of ROS-generating nanozymes for cancer therapy.

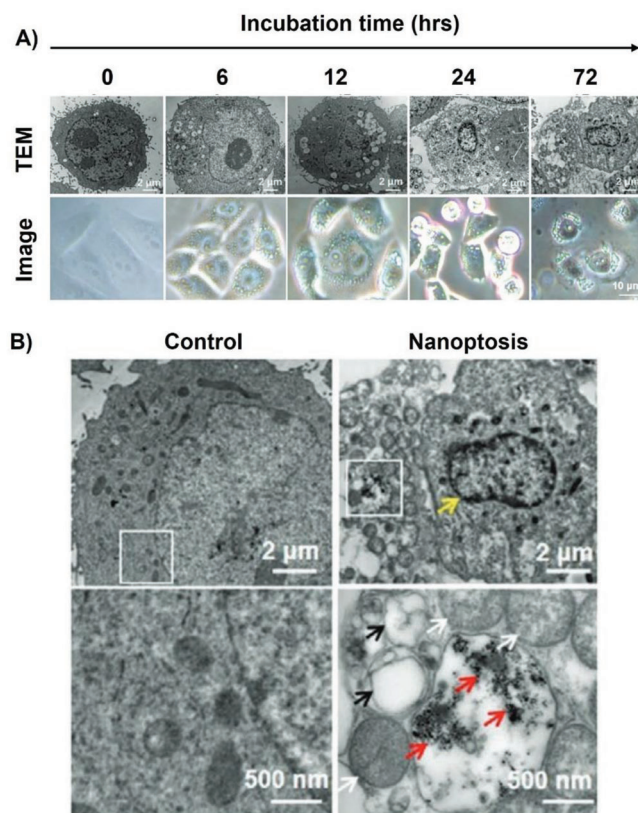| Nanozyme formulation	Treatment modality	Tumor model	Reference
HNPs@PPy	Photothermal therapy	4T1 tumor-bearing mice	[142]
C-NFs@Dox	ROS-facilitated treatment of therapy-resistant tumor	MCF-7/ADR tumor-bearing mice	[136]
PEGylated Pd SAzyme	Photothermal therapy	BALB/c mice with 4T1 xenograft	[143]
Fe_3O_4 NR(D2)@GOx	Multi-enzyme catalysis, magnetic field-based platform	4T1 tumor-bearing BALB/c mice	[144]
$NCeO_2$-PEI-MoS_2	Photothermal therapy	MDA-MB-231 breast cancer cells	[68]
GOx@Pd@ZIF-8	Synergistic anticancer activity that blocks glucose metabolism and produces ROS	Human lung adenocarcinoma A549-bearing Balb/c nude mice	[145]
PCF-a Nes	Dual modal cancer therapy	4T1 tumor-bearing mice	[146]
SAFe-NMCNs	Photothermal-augmented nanocatalytic therapy	MCF-7 tumor-bearing mice	[147]
MS-ICG@MnO_2@PEG	Photodynamic and chemodynamic therapy	4T1 tumor-bearing mice	[148]
CoO@AuPt	Chemodynamic therapy	4T1 breast tumor xenografts	[149]
Pd SAzyme	Mild-temperature PTT	BALB/c mice with 4T1 xenografts	[143]
AMP NRs	PTT-ECDT therapy	4T1 tumor-bearing mice	[107]
Au@HCNs	Catalytic–photothermal therapy	CT26 tumor-bearing mice	[78]
BON nanospheres	Multi-modal therapy	Mice bearing 4T1 tumors	[150]
Fe@Fe_3O_4@Cu_2–xS	Nanozyme based therapy	BALB/c mice with 4T1 xenografts	[151]
SnS_2@Fe_3O_4 NPs	RT and CDT	BALB/c nude mice with HeLa cells	[152]
Magnetic hydrogel nanozyme	Hyperthermia and catalytic therapy	4T1 breast tumor xenograft on BALB/c mice	[153]
Au-FeSAzyme	PTT	Oesophageal squamous tumor-bearing nude mice	[154]

therapeutic effect of Fe_3O_4 nanozymes toward the malignant tumor. This study also identified the inhibition of tumor growth in nanozyme treated female BALB/c wild-type mice implanted with murine carcinoma cells compared with controls treated with phosphate buffered saline alone.[141]

Apart from Fe-based POD-like nanozymes, many other nanozymes that induce ROS production have been explored as anti-cancer agents. Boron oxynitride (BON) nanostructures were designed to undergo degradation in an aqueous solution forming boric acid and $NH_4B_5O_8·4H_2O$, indicating the suitability of using these nanostructures as nanomedicines owing to biodegradability and lack of long-term toxicity.[150] The catalytic potency of BON is based on the generation of hydroxyl radicals measured using a fluorescent 7-hydroxycoumarin assay. The BON nanostructures reduced the viability of 4T1 cancer cells by 82% after treatment for 48 h by generating cytotoxic hydroxyl radicals. Microscopic studies indicated the reduction in cell density and alterations in the cell morphology with the increase in BON concentration. These BON could inhibit tumor growth by 97% after 14 days of treatment when compared with the PBS control samples.[150]

Cobalt-doped Fe_3O_4 (Co@Fe_3O_4) nanozymes were found to exhibit stronger peroxidase activity than Fe_3O_4 nanozymes. Lower doses of Co@Fe_3O_4 nanozymes catalyzed H_2O_2 efficiently and displayed promising in vitro and in vivo tumor inhibition efficacy.[82] Porous nanorods of ceria exhibited robust POD-like activity and were used to detect CA15-3, a biomarker of breast cancer.[89a] A spherical nanozyme system (Au@HCNs) consisting of a single gold nanoparticle core and porous carbon shell attained the yolk–shell structure and exhibited peroxidase-like activity with ROS generation activity for tumor annihilation.[78] The biodistribution of Au@HCNs in tumor-bearing mice indicated that the targeting efficiency of Au@HCNs to tumor cells was rel-

atively high. The improvement in ROS production was achieved by irradiation with 808 nm and associated photothermal heating.

Radiotherapy and chemotherapy are conventionally employed for cancer treatment, but the clinical efficacy of these therapies can be significantly impaired by interference from the tumor microenvironment. Thus, recent research in cancer therapy has explored stimulus-responsive and targeted cancer therapies, along with strategies for altering the tumor microenvironment. For instance, PDT employs photosensitive nanoparticles that generate ROS for catalytic cancer therapy under light irradiation. However, light can only penetrate short distances in the human body, which makes PDT unviable for deep-seated tumors. Zhong et al. reported $PtCu_3$ nanocages which can act as sonosensitizers and can efficiently generate ROS under ultrasound irradiation.[155] Ultrasound radiation can penetrate depths up to 10 cm in the human body. Thus, sonodynamic chemotherapy may be more effective for the treatment of deep-seated tumors. The synthesized $PtCu_3$ nanocages mimicked the biocatalytic function of horseradish peroxidase for the conversion of endogenous H_2O_2 into reactive hydroxyl radicals under acidic conditions and glutathione peroxidase activity (GPx) for oxidation of glutathione (GSH) into glutathione disulfide (GSSG).[155] The high concentration of GSH in tumor cells is one of the main reasons for the reduction of efficacy of conventional chemotherapy because GSH consumes ROS by getting oxidized to GSSG and depletes the effective concentration of ROS available for chemotherapy. $PtCu_3$ nanozymes reduced GSH levels through GPx activity and generated hydroxyl radicals through peroxidase-like activity. The most remarkable aspect of the synthesized $PtCu_3$ nanozyme was that it exhibited enhanced peroxidase activity under ultrasound irradiation and high absorption of near-infrared radiation and X-ray attenuation, allowing cancer imaging through photoacoustic and computed

**ADVANCED
SCIENCE NEWS**

www.advancedsciencenews.com

**ADVANCED
HEALTHCARE
MATERIALS**

www.advhealthmat.de

Figure 4. Distinct morphological and biological characteristics of a novel form of cell death termed nanoptosis induced by peroxidase-mimicking nanozymes: A) Condition of HepG2 cells after exposure to Fe_3O_4 nanozyme for different duration and B) comparison of nanoptosis with PBS buffer treated HepG2 cells; the region in the white box is depicted in lower panels, the yellow arrow points toward chromatin condensation, margination, and nucleolus disintegration, black arrows point toward the formation of monomembrane vesicles, white arrows point toward swelling of mitochondria and vacuolation, and red arrows point toward internalization of Fe_3O_4 nanozymes in lysosomes. Reproduced with permission.[141] Copyright 2020, Wiley-VCH GmbH.
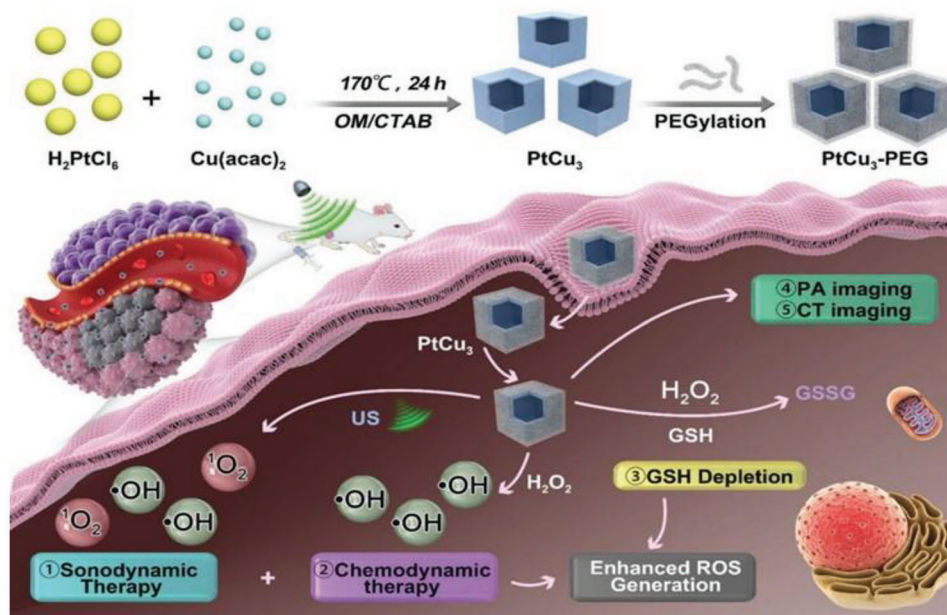
tomography imaging.[155] The functions and therapeutic actions of the highly effective $PtCu_3$ nanozymes are schematically illustrated in **Figure 5**.

Many other nanomaterials have been examined for use in cancer therapy with peroxidase-like activity, particularly MOFs. The rate of H_2O_2 generation in HeLa cells (cancer cells) was identified to be 4.81 times higher than in healthy NIH-3T3 cells. MOF-based nanozymes exhibit great versatility in fine-tuning the antitumor activity because they allow customization of both the metal centers and the constituent linker molecules. For instance, an iron-based MOF was synthesized hydrothermally, where some of the Fe^{3+} centers in the unit cell were partially reduced to Fe^{2+} centers. The metal node modification imparted a redox activity to the modified MOF with the ability to produce cytotoxic hydroxyl radicals in cells.[156] In addition, the MOF exhibited the capability for the controlled release of iron ions under an acidic ex vivo environment. Thus, both iron ions in the solution and in MOF structure reacted with H_2O_2 and increased ROS levels inside HeLa cells.[156] All these advancements highlight the possibilities of de-

veloping peroxidase-mimicking nanozymes for cancer theranostics.

Different strategies have also been developed to optimize nanozyme activity after it enters the target cell. Fan and co-workers prepared nitrogen-doped porous carbon nanospheres (N-PCNSs) and identified that they exhibited multiple enzyme-like capabilities, that is, oxidase-like, peroxidase-like, superoxide dismutase-like and catalase-like for regulation of ROS inside the tumor cells as shown in **Figure 6**A. Nitrogen doping was essential for controlling the enzymatic properties of porous carbon nanospheres (PCNSs) and subsequent regulation of ROS generation in cells.[157] Two different types of synthesized N-PCNSs-3 (3 h carbonization) and N-PCNSs-5 (5 h carbonization) inhibited HepG2 cell viability and exhibited toxic effects like those observed for H_2O_2.[157] Fluorescence imaging of PCNs indicated that mitochondrial membrane potential (MMP) malformed when added with N-PCNSs-3 and N-PCNSs-5, while no such effects were observed upon incubation with PCNSs, which confirmed the beneficial effect of N-doping for triggering apoptotic cascades in cells. A tenfold increase in DCFH-DA staining was detected after treatment of HepG2 cells with N-PCNSs-3, indicating ROS induction.[157] Delivery of ROS inducers to the target cell is another critical issue in tumor therapy. To achieve this, heavy chain ferritin (HFn) was conjugated with N-PCNSs via activation of carboxyl groups of N-PCNSs to react with the amino functionality of HFn. The internalization and lysosomal co-localization of HFn-N-PCNSs-3 was ≈23-fold higher than that of N-PCNSs-3, indicating the potential of HFn in targeting tumor cells and initiating ROS production in lysosomes as schematically illustrated in Figure 6B. The tumor growth was completely arrested within 5 days post-treatment in the group of BALB/c nude mice bearing human HepG2 tumor and treated with HFn-N-PCNSs-3 when compared with other groups injected with HFn-PCNSs, HFn or PCNSs (Figure 6C).

Multifunctional nanoplatforms have attracted substantial consideration as tumor therapeutic agents. The overexpression of H_2O_2 which is a typical characteristic of TME is commonly exploited to trigger the release of active drugs in chemotherapy.[158] In addition to chemotherapy, techniques like PDT and sonodynamic therapy also rely on this method to generate endogenous O_2 for oxygen-dependent tumor therapies. However, the lower intra-tumoral H_2O_2 concentration may be insufficient to achieve a reasonable therapeutic effect. In a combinatorial approach, a chlorin e6 (Ce6)-loaded peroxidase-mimicking MOF subsequently coated with hyaluronic acid (HA) was used to generate ROS. The resultant hydroxyl radicals and O_2 were used in chemodynamic therapy. The enhanced photodynamic therapy was also achieved by a Ce6-mediated photochemical effect, indicating cascade reactions suitable for tumor therapy. Therefore, a combined chemo-photodynamic therapy approach could be achieved for cancer treatment.[159] Zhu et al. developed a composite core shell-structured nanozyme (MS-ICG@MnO_2@PEG) as a photodynamic/chemodynamic therapeutic agent for ROS-mediated cancer treatment. The nanosystem catalyzed H_2O_2 to produce O_2 and generated hydroxyl radicals and enhanced both photodynamic and chemodynamic therapies. The core–shell nanosystems induced the generation of ROS in 4T1 tumor cells by affecting the mitochondrial function, thereby killing the cancer cells. In 4T1-tumor bearing mice, the nanosystems appeared to

**ADVANCED
SCIENCE NEWS**

www.advancedsciencenews.com

**ADVANCED
HEALTHCARE
MATERIALS**

www.advhealthmat.de

Figure 5. Schematic illustration of the multiple enzyme mimic activity of $PtCu_3$ nanocages and its use in sonodynamic chemotherapy. $PtCu_3$ nanozyme exhibited fivefold benefits such as enhanced peroxidase activity under ultrasound irradiation, generation of reactive oxygen species due to peroxidase activity, glutathione peroxidase activity for glutathione depletion, high near-infrared absorption for photoacoustic imaging, and X-ray attenuation for computer tomography imaging. Reproduced with permission.[155] Copyright 2019, Wiley-VCH GmbH.

be selectively accumulated at the tumor site and inhibited tumor growth providing a potential platform for ROS-based cancer treatment by enhancing PDT and CDT.[148]

One of the greatest challenges for in vivo application of nanozymes (and all other chemotherapeutics) for cancer treatment is site-selective delivery to cancerous cells to avoid side effects. It is well established that Fe_3O_4 nanoparticles exhibit both peroxidase and catalase activity in an acidic and basic environment. Therefore, it is necessary to tune the peroxidase activity while the catalase activity needs to be inhibited as it would remove ROS required for ROS-related treatment.[157] The nanozyme-based targeting system $Ag_2S@Fe_2C$-DSPE-PEG-iRGD displayed notable intracellular uptake, good fluorescence, and an increase in ROS production in 4T1 cells. The improved therapeutic performance was achieved when $Ag_2S@Fe_2C$-DSPE-PEG-iRGD were combined with bevacizumab during the treatment in 4T1 breast cancer-bearing mice. The excretion of the nanosystem was rapid, showing the potential of nanomedicines in breast cancer treatment.[134] Single-atom nanozymes (SAEs) have also been explored for the treatment of cancer because single atoms exhibit high catalytic activities and efficiencies for H_2O_2 conversion in the slightly acidic tumor microenvironment (TME) into cytotoxic hydroxyl radicals (•OH).[143,160] Zhu et al. synthesized single palladium atoms on carbon substrates, followed by encapsulation in agarose hydrogels along with the chemotherapeutic agent camptothecin (CPT). When the composite was irradiated with an 808 nm-laser, the photothermal effect induced by palladium single atoms resulted in localized heating enabling hyperthermia cancer treatment. In addition, CPT contributed to the termination of the tumor cells by increasing intratumoral H_2O_2 production through activating nicotinamide adenine dinucleotide phosphate oxidase. The peroxidase activity of synthesized nanozymes

converted H_2O_2 into cytotoxic hydroxyl radicals for tumor cell death. A schematic for the developed cancer treatment employing a synergistic combination of photothermal therapy, chemotherapy, and nanozyme-driven catalytic therapy is depicted in **Figure 7A**. Light-induced decomposition of the agarose hydrogel to release constituent elements and the mechanism of cytotoxic hydroxyl radical generation is shown in Figure 7B. The study provided strong evidence that the introduction of oxidative stress along with photothermal therapy can result in an effective cancer treatment modality without obvious toxic effects.[161]

In summary, nanozyme driven ROS generation for tumor suppression can be achieved using a variety of strategies and nanomaterials. Since nanozymes can affect the regulation of cellular redox levels, they can promote apoptosis in cancer cells. Furthermore, the efficacy of cancer treatments such as photothermal, photodynamic, sonodynamic, chemo- and radiotherapy can be enhanced using ROS-generating nanozyme systems. The synergistic effect of other cancer treatment modalities and new nanozyme capabilities could alleviate the problems associated with conventional treatments and improve therapeutic effects.

6.2. Hypoxia-Relieving Nanozymes for Cancer Therapy

Hypoxia is a characteristic feature of the tumor microenvironment linked to tumor progression, angiogenesis, metastasis, resistance, and recurrence, rendering conventional cancer treatment approaches ineffective over time.[12,162] Innovative strategies have been utilized to relieve hypoxia for the effective treatment of cancer. For instance, a wide range of oxygen-carrying and oxygen-generating nanomaterials, such as metal oxides, carbon-based nanomaterials and polymeric materials, have been widely

2300768 (15 of 28)
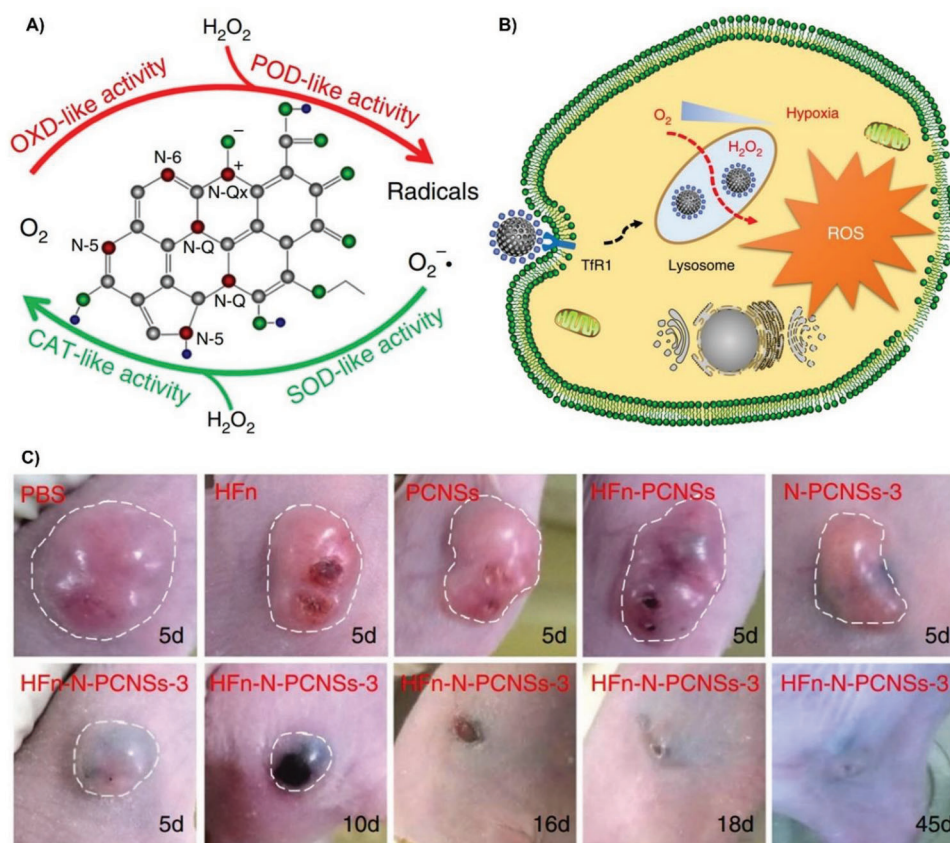
Figure 6. A) Schematic representation of a nitrogen-doped carbon-based nanozyme, termed N-PCNSs-3, which exhibited multiple enzyme-like catalytic activities, that is, oxidase-, peroxidase-, superoxide dismutase- and catalase-like properties. B) Schematic representation of ferritin-mediated specific delivery of N-PCNSs through the lysosomal pathway for ROS generation and tumor cell apoptosis and C) morphology of tumors and the deterioration after treatment with different types of HFn-N-PCNSs-3 nanozymes and treatment durations. Reproduced under the terms of the CC-BY license.[157] Copyright 2018, the Authors. Published by Springer Nature.

explored for enhanced tumor oxygenation.[22,28,163] Nanozymes have recently received wide attention for combinatorial cancer therapy modalities. The efficacy of these nanozyme systems depends upon their size, shape, composition, and surface area.[164] For hypoxia relief, catalase-mimicking nanozymes become most important for catalyzing the decomposition of H_2O_2 in cancer cells. Ultrasmall iridium nanocrystals (IrNCs) with inherent catalase activity were encapsulated in liposomal carriers, obtaining Ir@liposome. The nanosystem exhibited passive tumor accumulation when injected intravenously into mice. These materials, when exposed to NIR laser decomposed endogenous H_2O_2 into oxygen, relieving tumor hypoxia. The radiosensitization capacity of Ir as a high Z element enhanced the effect of cancer radiotherapy.[165] Porous Pt nanoparticles also displayed an enhanced effect when combined with radiotherapy. This was based on the benefits of the high atomic number to enhance the radiation dose and combine it with the oxygen generation capacity of the nanoparticles.[163] Furthermore, to strengthen the efficacy of PDT, MOFs integrated with photosensitizers were decorated with Pt nanozymes with catalase-like activity to facilitate the formation of $^1O_2$ at a hypoxic tumor site from H_2O_2.[26]

Romero and co-workers developed ultrasmall manganese ferrite nanoparticles with catalase-like activity with unparalleled tu-

mor growth inhibition in a breast cancer murine model along with potential as MRI contrast agents.[166] Besides, Li and colleagues designed the Fe^{3+} nanovesicles Fmoc-Cys/Fe@Pc and Fmoc-Cys/Fe@Pc/ACF that have the ability to ameliorate tumor hypoxic conditions by the transformation of H_2O_2.[63] The photosensitizing activity of the released zinc(II) phthalocyanine (Pc)-based photosensitizer was augmented and the nanovesicle decorated with the hypoxia-inducible factor 1 (HIF-1) inhibitor acriflavine (ACF) revealed higher in vitro and in vivo photodynamic activities than Fmoc-Cys/Fe@Pc, signifying the cooperative effect of ZnPc and ACF.

Metal oxide-based nanozymes have also demonstrated catalase-like activity to overcome tumor hypoxia. Bi_2Se_3–MnO_2@BSA nanocomposites were fabricated to trigger the decomposition of tumor endogenous H_2O_2 to overcome hypoxia-associated radioresistance. Bi_2Se_3 nanodots acted as radiosensitizers to increase the local radiation dosage because of their strong X-ray attenuation ability, and MnO_2 with catalase-like activity increased the oxygen concentration in tumor.[20] Wang and co-authors developed a multifunctional nanozyme for combinatorial cancer therapy by embedding tungsten disulfide quantum dots (WS_2 QDs) into mesoporous polydopamine nanosponges (MPDA NSs) and subsequent functionalization
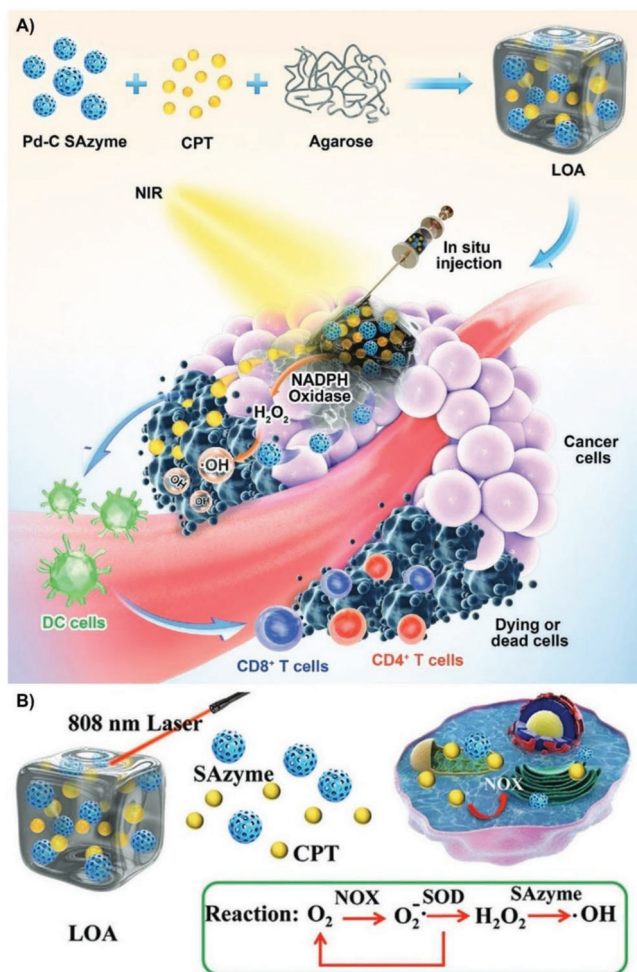
Figure 7. A) Schematic representation of H_2O_2 self-producing single-atom nanozyme hydrogels as light-controlled oxidative stress amplifiers for enhanced synergistic therapy, and B) representation of 808 nm-laser induced release of CPT and SAEs and hydroxyl radical generation. Reproduced with permission.[161] Copyright 2022, Wiley-VCH GmbH.

with manganese dioxide (MnO_2) nanosheets as shown in **Figure 8**A.[167] The developed nanozyme exhibited photothermal activity and decomposed H_2O_2 to relieve tumor hypoxia for oxygen-sensitized photo radiotherapy. In addition, the developed nanozymes acted as excellent contrast agents for T_1-weighted magnetic resonance (MR) imaging, computed tomography (CT) imaging and multispectral optoacoustic tomography imaging (MSOT). For instance, Figure 8B depicts the in vivo MSOT images of the internalization of MPDA-WS_2@MnO_2 nanozymes in tumor cells with increasing treatment time. Figure 8C depicts the improvement in contrast in CT imaging using developed nanozymes which allowed the detection of the presence of nanozymes in tumor cells 12 h after intravenous injection. Figure 8D depicts the improvement in contrast in MR imaging after the injection of nanozyme. The photothermal capability of nanozyme was characterized using thermal imaging, as indicated in Figure 8E. The rise in temperature at the tumor site after irradiation with an 808 nm-NIR laser induced irreversible

cancer tissue necrosis. The in vivo studies on different groups of tumor-bearing mice confirmed the inhibition of tumor growth when treated with MPDA-WS_2@MnO_2 nanozymes combined with radio and phototherapy.[167] Catalase-mimicking MOF nanosystems exhibited enhanced radiotherapy in hypoxic tumors and were found to prevent cancer recurrence.[19]

Noble metal nanosystems that mimic catalase to generate O_2 for tumor oxygenation are also widely investigated due to their strong NIR absorption and the potential to be used as photothermal agents for light conversion to heat in photothermal therapy.[168] The opportunity to design nanomaterials as nanotheranostic platforms for photothermal therapy using NIR-II light is widely used due to its deeper tissue penetration.[169] The photosensitizer chlorin e6 (Ce6) was covalently linked to platinum nanoparticles using the polymer NH_2-PEG-HS as a tool for PDT/PTT cancer therapy. The selective accumulation at the target site and circulation time in blood was achieved by modifying PEG, leading to stability and biocompatibility in physiological conditions. The catalase-mimicking capacity of Pt-Ce6 ameliorated the problem of tumor hypoxia by enhancing the synergistic effect of PDT and PTT.

Palladium nanosystems with catalytic activities have been extensively studied, including bimetallic systems, by developing surfaces to increase the number of catalytically active sites and adjusting the crystallinity. To obtain highly active catalase-mimicking nanozymes, a carboxyl-modified zinc phthalocyanine (ZnPc) loaded on Pd@TiO_2 (PTZC) increased the disproportionation of endogenous H_2O_2 by eightfold when compared to Pd NS and thereby reduced tumor hypoxia by generating enough O_2 driving PTZC migration to augment the synergistic therapeutic effects of PDT and PTT against hypoxic tumor both in vitro and in vivo.[28] This indicates that the interaction between nanozymes and the cell surface should be carefully considered and optimized to enable better in vivo activity. Moreover, the synergistic therapeutic mechanism needs to be systematically assessed to capitalize on the full therapeutic efficiency and minimize any undesirable side effects. Single-atom nanocatalysts with isolated active metal centers attached to solid support have displayed high catalytic activity and stability, which could present a useful strategy for cancer drug development due to the abundance of active sites.[170] Wang et al. developed single-atom nanozymes wherein Ru was incorporated into a $Mn_3[Co(CN)_6]_2$ MOF which was used as a supporting material. Self-assembly of Ce6 as a photosensitizer encapsulated by biocompatible poly-vinylpyrrolidone (PVP) polymer produced the uniform single-atom enzyme OxgeMCC-r SAE. The 4T1 cells treated with OxgeMCC-r SAEs exhibited an enhanced ROS stress level as compared with the group treated with $Mn_3[Co(CN)_6]_2$-Ce6 (MCC) nanoparticles. The in vivo PDT of OxgeMCC-r SAE was carried out on 4T1 tumor-bearing mice, and the average weight of tumor tissues obtained by anatomy for the group treated with OxgeMCC-r was the lowest at only 0.19 g. The therapeutic efficiency achieved by OxgeMCC-r SAE in comparison with the MCC group indicated the synergistic effect owing to the upsurge of O_2 for self-sustained photodynamic therapy.[171]

Another pertinent issue when using nanozymes synthesized for improving cancer treatment efficacy by modifying hypoxia is its clearance in vivo and catalytic stability. The ultrasmall Au NCs-ICG as nanozymes have been reported to enhance PDT and RT
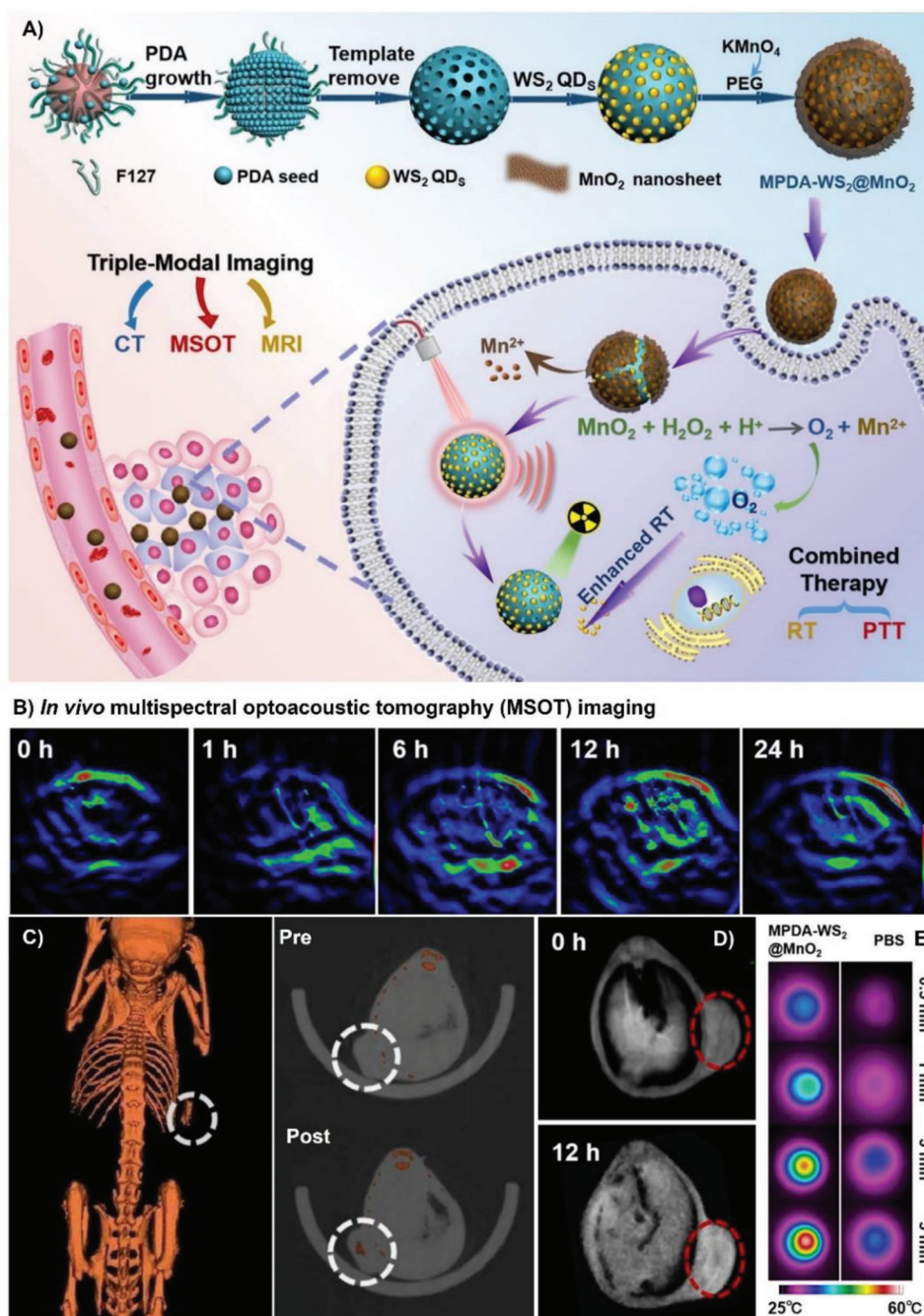
Figure 8. A) Schematic illustration of the synthesis of MPDA-WS$_2$@MnO$_2$ nanozymes and their application in oxygen-sensitized radiotherapy by ameliorating tumor hypoxia. B) In vivo multispectral optoacoustic tomography (MSOT) imaging capturing the internalization of nanozymes in tumor cells with time. C) Computed tomography imaging of tumor in mice before and after intravenous injection of MPDA-WS$_2$@MnO$_2$ nanozymes, white circles depict the location of the tumor, the concentration of nanozymes in tumor cells is evident from CT imaging. D) T1-weighted in vivo magnetic resonance images of the tumor before and after injection of MPDA-WS$_2$@MnO$_2$ nanozymes, a higher concentration of Mn in the tumor after injection is evident from the increase in intensity. E) Thermal images of the control sample (PBS-treated) and MPDA-WS$_2$@MnO$_2$ nanozymes aqueous dispersions after irradiation with a NIR laser for 5 min. Reproduced with permission.[167] Copyright 2019, Elsevier.

in which large amounts of O$_2$ were produced by adding Au NCs-ICG (50 μM) to H$_2$O$_2$ solutions. The singlet oxygen generation efficacy of Au NCs-ICG nanozymes was improved significantly in the presence of H$_2$O$_2$. Furthermore, Au NCs-ICG nanozymes decomposed intracellular H$_2$O$_2$ to O$_2$ by enhancing PDT in liv-ing cells. The tumor oxygen saturation increased rapidly from ≈2.7% to ≈26.7% when Au NCs were intra-tumorally injected into the 4T1 tumor-bearing mice for 1 h, indicating superior catalytic activity in vivo. The Au NCs-ICG nanozymes were mainly accumulated in the liver, kidneys, and tumor, confirming that

ADVANCED
SCIENCE NEWS
www.advancedsciencenews.com

ADVANCED
HEALTHCARE
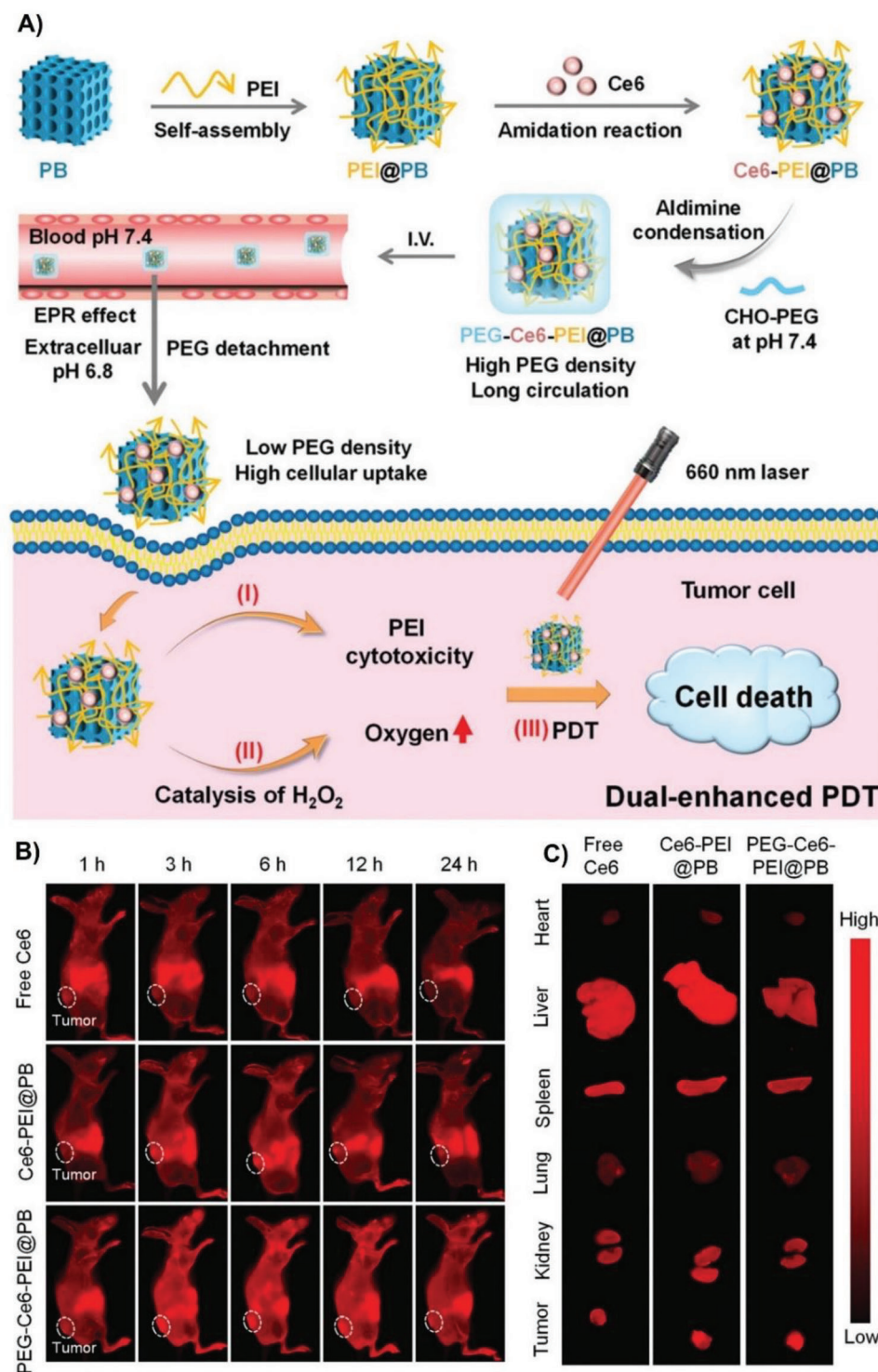**MATERIALS**
www.advhealthmat.de
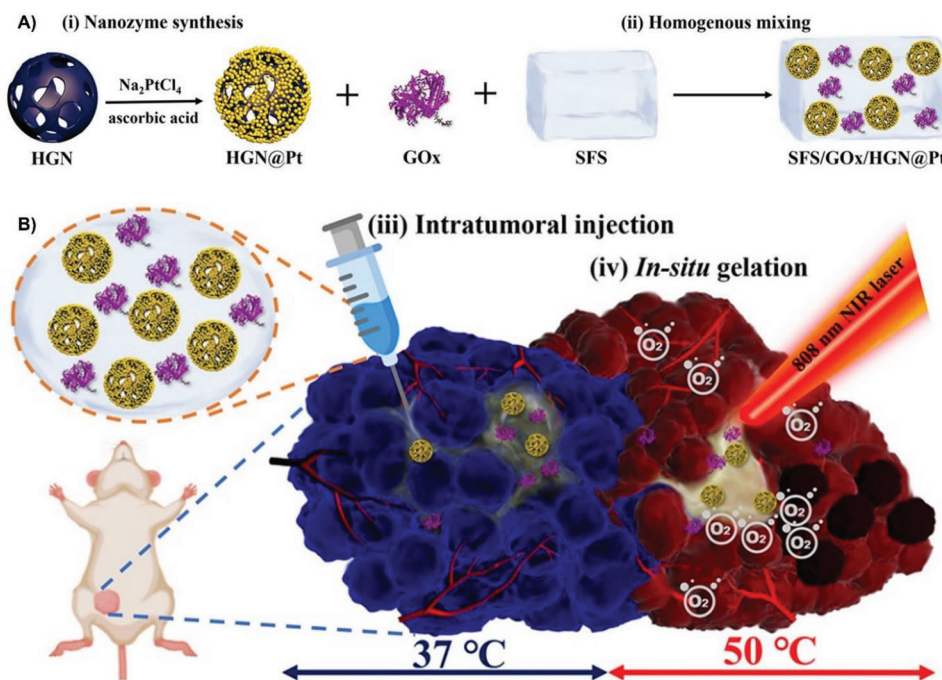
Figure 9. A) Schematic illustration of the synthesis of SFS/GOx/HGN@Pt nanozyme consisting of an enzyme-based silk fibroin hydrogel (SFS) matrix, natural enzyme glucose oxidase (GOx), and hollow Ag–Au metallic cages decorated by Pt nanoparticles (HGN@Pt). B) Schematic illustration of the mechanism of cancer therapy involving intravenous injection of the nanozyme, in situ condensation of hydrogel solution into a gel under light irradiation and heating of cancerous tissues generated by the photothermal effect. Reproduced with permission.[174] Copyright 2021, American Chemical Society.

ultrasmall Au NCs-ICG nanozymes could be efficiently cleared from the body through the kidneys minimizing the risks associated with treatment. The tumor-bearing mice that received Au NCs-ICG were cured without relapse, and the survival period of the mice was more than 39 days. Additionally, the efficiency of a combination of Au NCs-ICG and RT was assessed by measuring tumor volumes in tumor-bearing mice, which indicated remarkable inhibition of tumor growth and extended survival.[106]

Attempts have been made to enhance the catalase-mimicking activity of nanoparticles. Core-shell or alloy-structured nanomaterials can introduce surface strain effects that can improve the catalytic activity of the nanomaterials.[172] Hollow materials have a significantly larger number of atoms on the surface compared to the bulk due to their higher surface area, which results in higher catalytic activities and better control in fine-tuning of the catalytic activity.[173] Wu et al. developed a self-sufficient hybrid nanozyme system consisting of Pt-decorated hollow Ag–Au trimetallic nanocages (HGN@Pt) and natural enzyme glucose oxidase (GOx), which were encapsulated in an enzyme-based silk fibroin hydrogel (SFS) precursor solution as shown in **Figure 9**A.[174] Catalase like-activity of these nanozymes was investigated by measuring changes in the O_2 concentration in a deoxygenated H_2O_2 solution in the absence and presence of nanocrystals. It was identified that the Pt coating and the intrinsically hollow structure provided several active sites on the nanozyme surface and the trimetallic composition yielded a high catalytic effect when compared with mono- and bimetallic systems. Oxygen concentration decreased with a decrease in pH value from 7.4 to 5.8. However, the O_2 concentration increased at pH 5.8 when compared to the H_2O_2 solution indicating the

potential of the nanozyme to overcome tumor hypoxia in relatively acidic microenvironments.[174] Moreover, the GOx component of the nanozyme led to glucose depletion in the acidic tumor microenvironment resulting in starvation of the tumor cells. In vitro antitumor activity studies revealed that treatment with SFG/GOx/HGN@Pt30 and exposure to illumination with a NIR laser triggered the death of the 4T1 cells. SFG/GOx/HGN@Pt30 also displayed photothermal ability, which increased the efficacy of the combined treatment as schematically illustrated in Figure 9B.[174] Therefore, meticulous design and combinatorial therapies have tremendous potential in safe and effective elimination of cancer from a patient's body. Similarly, holey Pd nanospheres (H-Pd NSs) were identified to exhibit tetra-functional therapeutic capabilities for photodynamic and photothermal therapies, hypoxia relief and imaging-guided cancer therapy.[173] Prussian blue nanoparticles (PBNPs) exhibit interesting properties, as catalase-mimicking enzyme, act as a ROS scavenger due to the high affinity for hydroxyl radicals (•OH) and have excellent photothermal conversion capabilities, as well as a good level of biocompatibility. Thus, many studies have explored the use of PBNPs as a PTT agent for cancer treatment.[175] It is well established that the combination therapy of PDT with another tumor treatment modality for regulating the tumor microenvironment results in high efficacy in cancer treatment.[176] In this context, Wang et al. developed a composite nanozyme consisting of polyethylene glycol, polyethyleneimine (PEI), photosensitizer Ce6, and Prussian blue nanoparticles to attenuate tumor hypoxia as schematically illustrated in **Figure 10**A.[176] The cytotoxicity of PEI was eased by PEGylation and the developed nanozymes displayed catalase-like activity for amplification of

2300768 (19 of 28)

**ADVANCED
SCIENCE NEWS**

www.advancedsciencenews.com

**ADVANCED
HEALTHCARE
MATERIALS**

www.advhealthmat.de

Figure 10. A) Schematic illustration of the synthesis and antitumor mode of action of PEG-Ce6-PEI@PB nanozymes consisting of polyethylene glycol, photosensitizer Ce6, polyethylenimine, and Prussian blue nanoparticles for dual-enhanced photodynamic therapy induced by modulation of the polyethyleneimine cytotoxicity and hypoxia relief. B) Fluorescence imaging to capture the time-dependent biodistribution of free Ce6, Ce6-PEI@PB, by dynamic Schiff base crosslinking in response to pH changes. The cellular uptake of PEG-Ce6-PEI@PB nanoparticles was enhanced through extracellular pH-triggered PEG detachment and PEG-Ce6-PEI@PB in mouse models bearing tumors. C) Ex vivo fluorescence images of major organs and tumors 24 h after treatment. Reproduced with permission.[176] Copyright 2022, Royal Society of Chemistry.

**ADVANCED
SCIENCE NEWS**

www.advancedsciencenews.com

**ADVANCED
HEALTHCARE
MATERIALS**

www.advhealthmat.de

PDT. Tumor growth was inhibited by cytotoxic $^1O_2$ and the photosensitizer Ce6 transformed abundant O_2 into singlet oxygen when irradiated with a laser. In vivo biodistribution studies investigated using fluorescence imaging, as shown in Figure 10B, clearly indicated that PEGylation of the Ce6-PEI@PB components resulted in better blood circulation and enhanced internalization of the nanozymes into cancer cells.[176] Ex vivo imaging of mouse organs revealed that compared to Ce6-PEI@PB, the concentration of PEG-Ce6-PEI@PB increased at the tumor site, but its concentration in the liver, kidney, and spleen decreased, as evident from Figure 10C. PEG coating appears to be beneficial for protecting PEG-Ce6-PEI@PB from sequestration by the mononuclear phagocyte system. Thus, PEG-Ce6-PEI@PB nanozymes exhibited good biocompatibility and enhanced PDT by alleviating tumor hypoxia.[176]

7. Progress of Nanozyme-Driven Cancer Therapies in Clinical Trials

Current generation cancer treatments often prove unsuccessful in effective management and treatment of cancer due to resistance to chemotherapeutic drugs, undesired side effects, and spread of cancer to other parts of body (metastasis). Thus, oncology is gradually moving away from monotherapies to combinatorial or hybrid therapies where different strategies to manage tumor work synergistically to achieve the desirable outcomes. The article detailed several examples of such combinatorial therapies where ROS generation or hypoxia relief using nanozymes was coupled with simultaneous diagnosis or different treatment modalities. Despite their promising future, nanozyme-based cancer monotherapies are still in the initial stages of development and yet to make it to the clinical trials. However, several clinical trials are currently ongoing on nanoparticle-driven cancer treatment and diagnosis modalities which are relevant to the development of nanozyme-based combinatorial cancer therapies. These clinical studies provide useful insights into which nanomaterials and strategies have been successful where others have failed.

Iron-oxide nanoparticles have been used in magnetic field induced hyperthermia therapy for cancer treatment and cancer diagnosis by magnetic resonance imaging (MRI).[177] NanoTherm is the most successful clinical trial employing iron oxide nanoparticles which received EU-wide regulatory approval for hyperthermia treatment of glioblastoma in 2011. NanoTherm is composed of aminosilane-coated superparamagnetic iron oxide nanoparticles (SPIONs) which were injected directly into tumorous cells.[178] An alternating magnetic field was used to induce selective heating in the nanozymes which led to programmed and non-programmed cell death. NanoTherm is currently in late-stage clinical trials in US and yet to receive FDA approval there. A recent study reported an improvement in survival rates in glioblastoma patients by up to 12 months using these NanoTherm particles.[179] The success of iron oxide nanoparticles in the NanoTherm trials is evidence to the potential of peroxidase-mimic iron oxide nanozymes in treatment of cancer which can also be synergistically coupled with hyperthermia treatment due to the paramagnetic properties of iron oxide nanozymes. Elevated temperatures generated in hyperthermia may also increase the peroxidase activity of iron oxide nanozymes. Besides their use in hyperthermia, iron-oxide nanoparticles also find use in cancer

diagnosis because of their ability to enhance the contrast in magnetic resonance imaging. For instance, Feridex, GastroMark, and ferumoxytol (Feraheme) have been approved by FDA as MRI contrast agents. However, some of these contrast agents have been discontinued and ongoing studies are looking for more effective MRI contrast agents.

Gold nanozymes have been actively pursued for cancer therapy because of their unique optical, photocatalytic, photothermal, and enzyme-mimicking properties with readily tunable size, shape, and surface chemistry. Several, clinical trials are currently ongoing which employ the photothermal properties of gold nanoparticles for termination of cancer cells.[180] For instance, silica coated gold nanoparticles (Aurolase and Auroshell) were investigated for photothermal ablation of malignant cancer in the head, neck (NCT00848042), and prostrate (NCT04240639, NCT02680535, and NCT04656678).[181] These nanoparticles were observed to selectively accumulate in the tumor via permeation and retention effect while localized heating was induced due to the photothermal effect in gold nanoshells by near infrared laser. In the ongoing phase I clinical trial CYT-6091, PEGylated gold nanoparticles (27 nm) were used for targeted delivery of recombinant human tumor necrosis factor alpha (rhTNF) to tumorous cells.[182] Functionalization of gold nanoparticles with rhTNF allowed delivery of rhTNF in quantities up to three times higher than native rhTNF without causing any toxic effects.[182] Another ongoing early phase I trial (NCT03020017) investigated the safety of small interfering RNA (siRNA) targeting Bcl2L12 and thiolated PEG functionalised gold nanoparticles NU-0129 in the treatment of recurrent glioblastoma. It was identified that BU-0129 nanoparticles passed through the blood-brain barrier where it reduced Bcl2L12 protein abundance by RNA interference.[183] These clinical trials showcase the multifunctionality and potential of gold nanozymes in cancer therapy which exhibit pH dependent peroxidase activities. Thus, gold-based multicomponent nanozyme formulations have tremendous potential in the development of hybrid cancer treatments where ROS generation can be combined with gold driven photothermal therapy, photodynamic therapy, and targeted drug delivery.

Besides combination of nanozymes with different treatment modalities, nanozyme systems can also be coupled with diagnostic agents for development of simultaneous diagnosis and therapy (theranostic) modalities. The only nanoparticle-based therapeutic agent which has proceeded to clinical trials for simultaneous detection of cancer using MRI imaging and treatment by radiotherapy is gadolinium nanoparticles. Till date 17 clinical trials have been performed on the use of gadolinium-based nanoparticles as MRI contrast agents and detection of different types of cancers such as brain metastases, gynecologic cancer, brain tumor, glioblastoma multiforme, prostate carcinoma, and so on.[177] Lanthanide ions, Gd^{+3}, are gradually replacing iron oxide nanoparticles as T_1 contrast agents in MRI due to their favorable properties of high magnetic moment, para-magnetism, and coordination with water.[184] The gadolinium-based MRI contrast agents can be classified into two families based on the structure of complexing agents, that is, ones using linear complexing agents such as MAGNEVIST, OMNISCAN, OPTIMARK, and MultiHance and others using macrocycles such as PROHANCE, GADAVIST, and DOTAREM. However, some of these complexes

**ADVANCED
SCIENCE NEWS**

www.advancedsciencenews.com

**ADVANCED
HEALTHCARE
MATERIALS**

www.advhealthmat.de

have exhibited unsatisfactory efficiencies and residual toxicities. Thus, latest studies have focused on inorganic nanoparticles such as AGuIX which are based on polysiloxane Gd-chelates. AGuIX is currently undergoing four clinical trials for radiotherapy. In phase I clinical trial NCT02820454, radiotherapy with AGuIX was investigated for treatment of multiple brain metastases stemming from lung cancer, melanoma, colon cancer, and breast cancer. AGuIX was able to pass through the blood-brain barrier and exhibited successful detection of all the metastases that can be detected by conventional T_1 MRI contrast agents. In another ongoing clinical trial NCT03308604, the safety and tolerability of radiotherapy and brachytherapy using cisplatin and AGuIX is being investigated for treatment of patients with advanced cervical cancer. The success in clinical trials employing Gd-based nanozymes result from their high radio sensitizing abilities at extremely low concentrations, precision in the location and quantification of the concentration of radiosensitizers, their ultrasmall size that guarantees renal elimination.[177,185] Radio enhancers are such high electron density materials which increase the efficacy of radiotherapy by better absorption of incident radiation and localized generation of reactive species without causing harm to surrounding tissues. Hensify (NBTXR3) are hafnium oxide nanoparticles developed by Nanobiotrix for radiotherapy of solid non-small cell tumors in lungs, prostate, head and neck, liver and esophageal pancreatic.[186] These nanoparticles are specifically designed for cellular uptake and reduced leakage to surrounding tissues by optimization of their size and surface properties. NBTXR3 reached phase I clinical trials in 2011 and subsequently progressed to phase II/III trials for treatment of soft tissue sarcoma in 2016 (NCT02379845).[187]

From the above discussion it is clear that iron oxide and gold nanozymes-based cancer treatments which are successful in laboratory studies may be quickly advanced towards clinical trials. However, more data needs to be first collected in laboratory studies to better understand the enzymology of artificial nanozymes. One of the major challenges for nanozyme-based therapies is the specific targeting of tumor cells because off-target activity of nanozymes may cause damage to normal cells and generate side effects. Thus, control of the physico-chemical properties of nanozymes and their surface functionalization are essential for imparting them tumor-targeting capabilities and high clinical efficacies. The use of high activity nanozymes can also prove problematic if they mimic the activity of multiple enzymes which may reduce treatment efficacies or restricts their use in treatment all together. More in-depth studies are also needed to analyze the in vivo absorption, distribution, metabolism, excretion, cytotoxicity, and biocompatibility of any new type of nanozyme systems because the size, composition, surface charge, and surface corona can affect their specificity and toxicity. Besides fine tuning the physico-chemical properties of nanozymes, TME still remains the final frontier which needs to be overcome or strategically leveraged by the next-generation nanozymes. The TME is extremely dynamic which changes even in response to its own activity. The activity of nanozymes and multi-component nanozymes for combinatorial therapies need to be evaluated and understood in the milieu of the TME because nanozymes actively engage with and modify the TME. A persistent challenge in development of therapeutic agents for cancer therapies is the time taken for lab studies to pre-clinical trials and collection of clinically relevant data which may run into several decades. The translation of nanozyme-based catalytic therapies from the laboratory to clinical research and to market is yet to be seen. However, smart nanozymes are rapidly emerging as the frontrunners in oncology as the next generation therapeutic agents for combinatorial cancer treatments.

8. Conclusions, Challenges, and Perspectives

Most cancer treatments fail or are ineffective due to low therapeutic efficiency, adverse side effects, or resistance from the complex tumor microenvironment (TME). Nanozymes are attractive therapeutic agents for alternative and combinatorial cancer therapies due to their unique features such as stable and tunable catalytic activity, versatility in design, synthesis, and functionalization, better tissue penetration, and accumulation. Smart nanozymes have disruptive potential in alternative cancer therapy because they can exploit the TME for in situ generation of reactive species or re-engineer the TME itself for effective termination of tumor cells. The surface of nanozymes can also be easily tailored using ligands for site specific delivery or loaded with drugs to achieve catalytic-drug therapy. This allows the possibility for development of novel synergistic cancer treatments wherein conventional cancer treatments are synergistically enhanced using nanozymes. In such hybrid treatments nanozymes can help bypass the acquired resistance induced by the repeated long-term use of the single treatment and synergistic gains can be achieved without off-target toxicity effects.

Despite their promising future, nanozyme-based cancer treatments still have limitations. First and foremost it is important to understand the specific catalytic mechanism of each nanozyme especially under TME conditions using standard in vitro and in vivo models. Important factors that govern the catalytic activity of enzymes such as Michaelis–Menten kinetics should be considered in the assessment of nanozymes for combination therapy. It may be challenging to dynamically maintain the nanozyme catalytic activity in an everchanging tumor microenvironment. Biosafety of these nanosystems is also critical because nanoparticle size, composition, surface charge, and surface corona can affect multiple parameters such as their specificity, stability, bioactivity, and toxicity. The required biosafety and specificity for nanozymes can be achieved using rational design and performance optimization with respect to material composition and structure. The translation of nanozyme-based catalytic therapies from the laboratory to clinical research and to market is yet to be seen. However, nanozymes can greatly contribute to oncology and can be used as effective therapeutic agents for standalone or combinatorial cancer treatments.

Supporting Information

Supporting Information is available from the Wiley Online Library or from the author.

Acknowledgements

2300768 (22 of 28)

the effective treatment of ovarian cancer—AIRXII000200". Distinguished professor S.B. expresses his gratitude toward his mentor and supervisor, the late Professor E. W. Abel, Exeter UK, for giving him the power of knowledge and mentorship to produce scientists for tomorrow.

Open access publishing facilitated by RMIT University, as part of the Wiley - RMIT University agreement via the Council of Australian University Librarians.

Conflict of Interest

The authors declare no conflict of interest.

Keywords

cancer, catalytic activities, nanotechnology, nanozymes, oncology, therapies, tumor microenvironments

[1] J. Ferlay, M. Colombet, I. Soerjomataram, D. M. Parkin, M. Piñeros, A. Znaor, F. Bray, *Int. J. Cancer.* **2021**, *149*, 778.

[2] W. H. Gmeiner, S. Ghosh, *Nanotechnol. Rev.* **2015**, *3*, 111.

[3] K. Bukowski, M. Kciuk, R. Kontek, *Int. J. Mol. Sci.* **2020**, *21*, 3233.

[4] W. M. Linehan, G. Bratslavsky, P. A. Pinto, L. S. Schmidt, L. Neckers, D. P. Bottaro, R. Srinivasan, *Annu. Rev. Med.* **2010**, *61*, 329.

[5] S. Lheureux, C. Gourley, I. Vergote, A. M. Oza, *Lancet* **2019**, *393*, 1240.

[6] a) J. M. Brown, in *Methods in Enzymology*, Vol. *435*, Academic Press, Cambridge, MA **2007**; b) H. Majeed, V. Gupta, *Adverse Effects of Radiation Therapy*, StatPearls Publishing, Treasure Island, FL **2022**; c) R. Shi, C. Liao, Q. Zhang, *Cells* **2021**, *10*, 678.

[7] S. R. Corrie, M. Plebanski, *Mol. Immunol.* **2018**, *98*, 28.

[8] a) D. Jiang, D. Ni, Z. T. Rosenkrans, P. Huang, X. Yan, W. Cai, *Chem. Soc. Rev.* **2019**, *48*, 3683; b) R. Mohamud, S. D. Xiang, S. Selomulya, J. M. Rolland, R. E. O'Hehir, C. L. Hardy, M. Plebanski, *Drug Metab. Rev.* **2014**, *46*, 176.

[9] M. Liang, X. Yan, *Acc. Chem. Res.* **2019**, *52*, 2190.

[10] J. Ma, J. Qiu, S. Wang, *ACS Appl. Nano Mater.* **2020**, *3*, 4925.

[11] a) H. Fei, J. Dong, Y. Feng, C. S. Allen, C. Wan, B. Volosskiy, M. Li, Z. Zhao, Y. Wang, H. Sun, P. An, W. Chen, Z. Guo, C. Lee, D. Chen, I. Shakir, M. Liu, T. Hu, Y. Li, A. I. Kirkland, X. Duan, Y. Huang, *Nat. Catal.* **2018**, *1*, 63; b) M. Wei, J. Lee, F. Xia, P. Lin, X. Hu, F. Li, D. Ling, *Acta Biomater.* **2021**, *126*, 15.

[12] Y. Zhang, Y. Jin, H. Cui, X. Yan, K. Fan, *RSC Adv.* **2019**, *10*, 10.

[13] H. Wang, K. Wan, X. Shi, *Adv. Mater.* **2019**, *31*, 1805368.

[14] N. M. Phan, T. L. Nguyen, J. Kim, *Tissue Eng. Regener. Med.* **2022**, *19*, 237.

[15] X. Zhu, N. Xu, L. Zhang, D. Wang, P. Zhang, *Eur. J. Med. Chem.* **2022**, *238*, 114456.

[16] a) S. Li, L. Shang, B. Xu, S. Wang, K. Gu, Q. Wu, Y. Sun, Q. Zhang, H. Yang, F. Zhang, L. Gu, T. Zhang, H. Liu, *Angew. Chem., Int. Ed. Engl.* **2019**, *58*, 12624; b) L. Zhu, Y. Dai, L. Gao, Q. Zhao, *Int. J. Nanomed.* **2021**, *16*, 4559.

[17] S. Khan, M. Sharifi, S. H. Bloukh, Z. Edis, R. Siddique, M. Falahati, *Talanta* **2021**, *224*, 121805.

[18] Y. Huang, J. Ren, X. Qu, *Chem. Rev.* **2019**, *119*, 4357.

[19] Y. Chen, H. Zhong, J. Wang, X. Wan, Y. Li, W. Pan, N. Li, B. Tang, *Chem. Sci.* **2019**, *10*, 5773.

[20] Y. Yao, P. Li, J. He, D. Wang, J. Hu, X. Yang, *ACS Appl. Mater. Interfaces* **2021**, *13*, 28650.

[21] M. Chang, Z. Hou, M. Wang, M. Wang, P. Dang, J. Liu, M. Shu, B. Ding, A. A. Al Kheraif, C. Li, J. Lin, *Small* **2020**, *16*, 1907146.

[22] R. Zhang, L. Chen, Q. Liang, J. Xi, H. Zhao, Y. Jin, X. Gao, X. Yan, L. Gao, K. Fan, *Nano Today* **2021**, *41*, 101317.

[23] L. Luo, L. Li, C. Cong, Y. He, Z. Hao, D. Gao, *Sci. China Mater.* **2020**, *64*, 1021.

[24] H. Wu, Q. Jiang, K. Luo, C. Zhu, M. Xie, S. Wang, Z. Fei, J. Zhao, *J. Nanobiotechnol.* **2021**, *19*, 203.

[25] Z. He, X. Huang, C. Wang, X. Li, Y. Liu, Z. Zhou, S. Wang, F. Zhang, Z. Wang, O. Jacobson, J. J. Zhu, G. Yu, Y. Dai, X. Chen, *Angew. Chem., Int. Ed. Engl.* **2019**, *58*, 8752.

[26] Y. Zhang, F. Wang, C. Liu, Z. Wang, L. Kang, Y. Huang, K. Dong, J. Ren, X. Qu, *ACS Nano* **2018**, *12*, 651.

[27] J. Xi, W. Wang, L. Da, J. Zhang, L. Fan, L. Gao, *ACS Biomater. Sci. Eng.* **2018**, *4*, 1083.

[28] C. Wang, Y. Li, W. Yang, L. Zhou, S. Wei, *Adv. Healthcare Mater.* **2021**, *10*, 2100601.

[29] Z. Nie, Y. Vahdani, W. C. Cho, S. H. Bloukh, Z. Edis, S. Haghighat, M. Falahati, R. Kheradmandi, L. A. Jaragh-Alhadad, M. Sharifi, *Arabian J. Chem.* **2022**, *15*, 41.

[30] H. Wang, J. Tao, C. Xu, Y. Tian, G. Lu, B. Yang, Z. Teng, *Nanoscale* **2022**, *14*, 9702.

[31] J. Wang, S. Gao, X. Wang, H. Zhang, X. Ren, J. Liu, F. Bai, *Nano Res.* **2022**, *15*, 2347.

[32] L. Hu, W. Sun, Y. Tang, S. Li, B. Zhang, X. Sun, W. Ji, L. Ma, H. Deng, S. Han, D. Zhu, *Carbon* **2021**, *176*, 148.

[33] Y. Zhao, B. Ding, X. Xiao, F. Jiang, M. Wang, Z. Hou, B. Xing, B. Teng, Z. Cheng, P. Ma, J. Lin, *ACS Appl. Mater. Interfaces* **2020**, *12*, 11320.

[34] L. Feng, B. Liu, R. Xie, D. Wang, C. Qian, W. Zhou, J. Liu, D. Jana, P. Yang, Y. Zhao, *Adv. Funct. Mater.* **2020**, *31*, 2006216.

[35] Z. Wang, G. Li, Y. Gao, Y. Yu, P. Yang, B. Li, X. Wang, J. Liu, K. Chen, J. Liu, W. Wang, *Chem. Eng. J.* **2021**, *404*, 125574.

[36] S. Dong, Y. Dong, B. Liu, J. Liu, S. Liu, Z. Zhao, W. Li, B. Tian, R. Zhao, F. He, S. Gai, Y. Xie, P. Yang, Y. Zhao, *Adv. Mater.* **2022**, *34*, 2107054.

[37] S. Gao, H. Lin, H. Zhang, H. Yao, Y. Chen, J. Shi, *Adv. Sci.* **2018**, *6*, 1801733.

[38] Y. Chong, X. Dai, G. Fang, R. Wu, L. Zhao, X. Ma, X. Tian, S. Lee, C. Zhang, C. Chen, Z. Chai, C. Ge, R. Zhou, *Nat. Commun.* **2018**, *9*, 4861.

[39] C. Wu, D. Xu, M. Ge, J. Luo, L. Chen, Z. Chen, Y. You, Y.-x. Zhu, H. Lin, J. Shi, *Nano Today* **2022**, *46*, 101574.

[40] C. Cao, H. Zou, N. Yang, H. Li, Y. Cai, X. Song, J. Shao, P. Chen, X. Mou, W. Wang, X. Dong, *Adv. Mater.* **2021**, *33*, 2106996.

[41] C. Fang, Z. Deng, G. Cao, Q. Chu, Y. Wu, X. Li, X. Peng, G. Han, *Adv. Funct. Mater.* **2020**, *30*, 1910085.

[42] Z. Yuan, X. Liu, J. Ling, G. Huang, J. Huang, X. Zhu, L. He, T. Chen, *Biomaterials* **2022**, *287*, 121620.

[43] C. Liu, J. Xing, O. U. Akakuru, L. Luo, S. Sun, R. Zou, Z. Yu, Q. Fang, A. Wu, *Nano Lett.* **2019**, *19*, 5674.

[44] B. Garg, T. Bisht, *Molecules* **2016**, *21*, 1653.

[45] F. Attar, M. G. Shahpar, B. Rasti, M. Sharifi, A. A. Saboury, S. M. Rezayat, M. Falahati, *J. Mol. Liq.* **2019**, *278*, 130.

[46] Z. Li, W. Liu, P. Ni, C. Zhang, B. Wang, G. Duan, C. Chen, Y. Jiang, Y. Lu, *Chem. Eng. J.* **2022**, *428*, 131396.

[47] J. Guo, Y. Wang, M. Zhao, *Sens. Actuators, B* **2019**, *297*.

[48] P. Khramtsov, M. Kropaneva, V. Bochkova, D. Timganova, D. Kiselkov, S. Zamorina, M. Rayev, *Colloids Interfaces* **2022**, *6*, 29.

[49] S. B. Bankar, M. V. Bule, R. S. Singhal, L. Ananthanarayan, *Biotechnol. Adv.* **2009**, *27*, 489.

[50] a) W. Zhen, Y. Liu, W. Wang, M. Zhang, W. Hu, X. Jia, C. Wang, X. Jiang, *Angew. Chem., Int. Ed. Engl.* **2020**, *59*, 9491; b) H. Zhou, T. Han, Q. Wei, S. Zhang, *Anal. Chem.* **2016**, *88*, 2976; c) N. J. Lang, B. Liu, J. Liu, *J. Colloid Interface Sci.* **2014**, *428*, 78.

[51] G. Vinothkumar, P. Arunkumar, A. Mahesh, A. Dhayalan, K. Suresh Babu, *New J. Chem.* **2018**, *42*, 18810.

[52] J. G. You, Y. W. Liu, C. Y. Lu, W. L. Tseng, C. J. Yu, *Biosens. Bioelectron.* **2017**, *92*, 442.

[53] L. Teng, X. Han, Y. Liu, C. Lu, B. Yin, S. Huan, X. Yin, X. B. Zhang, G. Song, *Angew. Chem., Int. Ed. Engl.* **2021**, *60*, 26142.

[54] K. H. Cheeseman, T. F. Slater, *Br. Med. Bull.* **1993**, *49*, 481.

[55] D. Harman, *Mutat. Res.* **1992**, *275*, 257.

[56] J. D. Crapo, T. Oury, C. Rabouille, J. W. Slot, L.-Y. Chang, *Cell Biol.* **1992**, *89*, 10405.

[57] Y. Sheng, I. A. Abreu, D. E. Cabelli, M. J. Maroney, A. F. Miller, M. Teixeira, J. S. Valentine, *Chem. Rev.* **2014**, *114*, 3854.

[58] S. Torbrugge, M. Reichling, A. Ishiyama, S. Morita, O. Custance, *Phys. Rev. Lett.* **2007**, *99*, 056101.

[59] a) W. He, Y. T. Zhou, W. G. Wamer, X. Hu, X. Wu, Z. Zheng, M. D. Boudreau, J. J. Yin, *Biomaterials* **2013**, *34*, 765; b) K. Korschelt, R. Ragg, C. S. Metzger, M. Kluenker, M. Oster, B. Barton, M. Panthofer, D. Strand, U. Kolb, M. Mondeshki, S. Strand, J. Brieger, M. Nawaz Tahir, W. Tremel, *Nanoscale* **2017**, *9*, 3952; c) J. Mu, X. Zhao, J. Li, E. C. Yang, X. J. Zhao, *J. Mater. Chem. B* **2016**, *4*, 5217; d) J. Dong, L. Song, J. J. Yin, W. He, Y. Wu, N. Gu, Y. Zhang, *ACS Appl. Mater. Interfaces* **2014**, *6*, 1959; e) Z. Miao, S. Jiang, M. Ding, S. Sun, Y. Ma, M. R. Younis, G. He, J. Wang, J. Lin, Z. Cao, P. Huang, Z. Zha, *Nano Lett.* **2020**, *20*, 3079.

[60] E. L. Samuel, D. C. Marcano, V. Berka, B. R. Bitner, G. Wu, A. Potter, R. H. Fabian, R. G. Pautler, T. A. Kent, A. L. Tsai, J. M. Tour, *Proc. Natl. Acad. Sci. U. S. A.* **2015**, *112*, 2343.

[61] I. v. Ossowski, G. Hausner, P. C. Loewen, *J. Mol. Evol.* **1993**, *37*, 71.

[62] a) L. Meng, Y. Cheng, S. Gan, Z. Zhang, X. Tong, L. Xu, X. Jiang, Y. Zhu, J. Wu, A. Yuan, Y. Hu, *Mol. Pharmaceutics* **2018**, *15*, 447; b) A. Z. Abbasi, C. R. Gordijo, M. A. Amini, A. Maeda, A. M. Rauth, R. S. DaCosta, X. Y. Wu, *Cancer Res.* **2016**, *76*, 6643; c) P. Prasad, C. R. Gordijo, A. Z. Abbasi, A. Maeda, A. Ip, A. M. Rauth, R. S. DaCosta, X. Y. Wu, *ACS Nano* **2014**, *8*, 3202.

[63] Y. Li, P. Sun, L. Zhao, X. Yan, D. K. P. Ng, P. C. Lo, *Angew. Chem., Int. Ed. Engl.* **2020**, *59*, 23228.

[64] Q. Chen, S. He, F. Zhang, F. Cui, J. Liu, M. Wang, D. Wang, Z. Jin, C. Li, *Sci. China Mater.* **2020**, *64*, 510.

[65] L. Gao, J. Zhuang, L. Nie, J. Zhang, Y. Zhang, N. Gu, T. Wang, J. Feng, D. Yang, S. Perrett, X. Yan, *Nat. Nanotechnol.* **2007**, *2*, 577.

[66] Y. Zhou, H. Sun, H. Xu, S. Matysiak, J. Ren, X. Qu, *Angew. Chem., Int. Ed. Engl.* **2018**, *57*, 16791.

[67] a) S. Mehla, P. R. Selvakannan, S. K. Bhargava, *Nanoscale* **2022**, *14*, 9989; b) S. Mehla, A. Kandjani, V. Coyle, C. J. Harrison, M. X. Low, R. B. Kaner, Y. Sabri, S. K. Bhargava, *ACS Appl. Nano Mater.* **2022**, *5*, 1873.

[68] C. Murugan, N. Murugan, A. K. Sundramoorthy, A. Sundaramurthy, *Chem. Commun.* **2019**, *55*, 8017.

[69] B. Ma, J. Han, K. Zhang, Q. Jiang, Z. Sui, Z. Zhang, B. Zhao, Z. Liang, L. Zhang, Y. Zhang, *J. Mater. Chem. B* **2022**, *10*, 1410.

[70] Y. Chen, Y. Yin, Y. Zhang, Y. Liu, J. Zan, C. Xie, Q. Fan, W. Huang, *Dyes Pigm.* **2021**, *191*, 109350.

[71] J. Li, W. Liu, X. Wu, X. Gao, *Biomaterials* **2015**, *48*, 37.

[72] Y. Chong, J. Huang, X. Xu, C. Yu, X. Ning, S. Fan, Z. Zhang, *Bioconjugate Chem.* **2020**, *31*, 1756.

[73] A. M. Alkilany, C. J. Murphy, *J. Nanopart. Res.* **2010**, *12*, 2313.

[74] a) G. Hou, J. Qian, M. Guo, W. Xu, J. Wang, Y. Wang, A. Suo, *Chem. Eng. J.* **2022**, *435*, 134778; b) J. Wang, J. Ye, W. Lv, S. Liu, Z. Zhang, J. Xu, M. Xu, C. Zhao, P. Yang, Y. Fu, *ACS Appl. Mater. Interfaces* **2022**, *14*, 40645.

[75] S. Li, W. Sun, Y. Luo, Y. Gao, X. Jiang, C. Yuan, L. Han, K. Cao, Y. Gong, C. Xie, *J. Mater. Chem. B* **2021**, *9*, 4643.

[76] M. Wang, M. Chang, P. Zheng, Q. Sun, G. Wang, J. Lin, C. Li, *Adv. Sci. (Weinh)* **2022**, *9*, 2202332.

[77] A. Zhang, S. Pan, Y. Zhang, J. Chang, J. Cheng, Z. Huang, T. Li, C. Zhang, J. M. de la Fuentea, Q. Zhang, D. Cui, *Theranostics* **2019**, *9*, 3443.

[78] L. Fan, X. Xu, C. Zhu, J. Han, L. Gao, J. Xi, R. Guo, *ACS Appl. Mater. Interfaces* **2018**, *10*, 4502.

[79] Z. Xu, J. Chen, Y. Li, T. Hu, L. Fan, J. Xi, J. Han, R. Guo, *J. Colloid Interface Sci.* **2022**, *628*, 1033.

[80] Q. An, C. Sun, D. Li, K. Xu, J. Guo, C. Wang, *ACS Appl. Mater. Interfaces* **2013**, *5*, 13248.

[81] a) S. Zanganeh, G. Hutter, R. Spitler, O. Lenkov, M. Mahmoudi, A. Shaw, J. S. Pajarinen, H. Nejadnik, S. Goodman, M. Moseley, L. M. Coussens, H. E. Daldrup-Link, *Nat. Nanotechnol.* **2016**, *11*, 986; b) X. Wang, T. Xiong, M. Cui, X. Guan, J. Yuan, Z. Wang, R. Li, H. Zhang, S. Duan, F. Wei, *Appl. Mater. Today* **2020**, *21*, 100827.

[82] Y. Wang, H. Li, L. Guo, Q. Jiang, F. Liu, *RSC Adv.* **2019**, *9*, 18815.

[83] B. Jiang, L. Yan, J. Zhang, M. Zhou, G. Shi, X. Tian, K. Fan, C. Hao, X. Yan, *ACS Appl. Mater. Interfaces* **2019**, *11*, 9747.

[84] S. Mehla, A. E. Kandjani, R. Babarao, A. F. Lee, S. Periasamy, K. Wilson, S. Ramakrishna, S. K. Bhargava, *Energy Environ. Sci.* **2021**, *14*, 320.

[85] G. Fu, W. Liu, Y. Li, Y. Jin, L. Jiang, X. Liang, S. Feng, Z. Dai, *Bioconjugate Chem.* **2014**, *25*, 1655.

[86] M. Gautam, K. Poudel, C. S. Yong, J. O. Kim, *Int. J. Pharm.* **2018**, *549*, 31.

[87] Z. H. Li, Y. Chen, Y. Sun, X. Z. Zhang, *ACS Nano* **2021**, *15*, 5189.

[88] W. Shen, G. Han, L. Yu, S. Yang, X. Li, W. Zhang, P. Pei, *Int. J. Nanomed.* **2022**, *17*, 1397.

[89] a) Z. Tian, J. Li, Z. Zhang, W. Gao, X. Zhou, Y. Qu, *Biomaterials* **2015**, *59*, 116; b) X. Xia, J. Zhang, N. Lu, M. J. Kim, K. Ghale, Y. Xu, E. McKenzie, J. Liu, H. Ye, *ACS Nano* **2015**, *9*, 9994; c) X. Hu, F. Li, F. Xia, X. Guo, N. Wang, L. Liang, B. Yang, K. Fan, X. Yan, D. Ling, *J. Am. Chem. Soc.* **2020**, *142*, 1636; d) J. Xie, X. Zhang, H. Jiang, S. Wang, H. Liu, Y. Huang, *RSC Adv.* **2014**, *4*, 26046; e) S. Ghosh, P. Roy, N. Karmodak, E. D. Jemmis, G. Mugesh, *Angew. Chem., Int. Ed. Engl.* **2018**, *57*, 4510; f) C. Wang, H. Wang, B. Xu, H. Liu, *View* **2020**, *2*, 20200045.

[90] a) N. Singh, M. A. Savanur, S. Srivastava, P. D'Silva, G. Mugesh, *Angew. Chem., Int. Ed. Engl.* **2017**, *56*, 14267; b) C. Ge, G. Fang, X. Shen, Y. Chong, W. G. Wamer, X. Gao, Z. Chai, C. Chen, J. J. Yin, *ACS Nano* **2016**, *10*, 10436.

[91] S. Liu, F. Lu, R. Xing, J. J. Zhu, *Chemistry* **2011**, *17*, 620.

[92] K. Jiang, D. A. Smith, A. Pinchuk, *J. Phys. Chem. C* **2013**, *117*, 27073.

[93] G. Tang, J. He, J. Liu, X. Yan, K. Fan, *Exploration* **2021**, *1*, 75.

[94] K. Fan, H. Wang, J. Xi, Q. Liu, X. Meng, D. Duan, L. Gao, X. Yan, *Chem. Commun.* **2016**, *53*, 424.

[95] J. Ren, N. Andrikopoulos, K. Velonia, H. Tang, R. Cai, F. Ding, P. C. Ke, C. Chen, *J. Am. Chem. Soc.* **2022**, *144*, 9184.

[96] P. T. Kutoka, T. A. Seidu, V. Baye, A. M. Khamis, C. T. q. Omonova, B. Wang, *OpenNano* **2022**, *7*, 100041.

[97] T. L. Whiteside, *Oncogene* **2008**, *27*, 5904.

[98] A. Patel, S. Sant, *Biotechnol. Adv.* **2016**, *34*, 803.

[99] Y. Kim, Q. Lin, P. M. Glazer, Z. Yun, *Curr. Mol. Med.* **2009**, *9*, 425.

[100] B. Muz, P. de la Puente, F. Azab, A. K. Azab, *Hypoxia* **2015**, *3*, 83.

[101] W. R. Wilson, M. P. Hay, *Nat. Rev. Cancer* **2011**, *11*, 393.

[102] A. L. Harris, *Nat. Rev. Cancer* **2002**, *2*, 38.

[103] N. A. Bhowmick, E. G. Neilson, H. L. Moses, *Nature* **2004**, *432*, 332.

[104] B. J. Moeller, R. A. Richardson, M. W. Dewhirst, *Cancer Metastasis Rev.* **2007**, *26*, 241.

[105] P. Vaupel, D. K. Kelleher, M. Hckel, *Semin. Oncol.* **2001**, *28*, 29.

[106] Q. Dan, D. Hu, Y. Ge, S. Zhang, S. Li, D. Gao, W. Luo, T. Ma, X. Liu, H. Zheng, Y. Li, Z. Sheng, *Biomater. Sci.* **2020**, *8*, 973.

[107] F. Liu, L. Lin, Y. Zhang, Y. Wang, S. Sheng, C. Xu, H. Tian, X. Chen, *Adv. Mater.* **2019**, *31*, 1902885.

[108] M. V. Liberti, J. W. Locasale, *Trends Biochem. Sci.* **2016**, *41*, 211.

**ADVANCED
SCIENCE NEWS**

www.advancedsciencenews.com

**ADVANCED
HEALTHCARE
MATERIALS**

www.advhealthmat.de

[109] V. Estrella, T. Chen, M. Lloyd, J. Wojtkowiak, H. H. Cornnell, A. Ibrahim-Hashim, K. Bailey, Y. Balagurunathan, J. M. Rothberg, B. F. Sloane, J. Johnson, R. A. Gatenby, R. J. Gillies, *Cancer Res.* **2013**, *73*, 1524.

[110] I. Marchiq, J. Pouysségur, *J. Mol. Med.* **2016**, *94*, 155.

[111] A. J. Levine, A. M. Puzio-Kuter, *Science* **2012**, *330*, 1340.

[112] J. B. Choi, J. H. Kim, H. Lee, J. N. Pak, B. S. Shim, S. H. Kim, *J. Agric. Food Chem.* **2018**, *66*, 9960.

[113] H. Deng, W. Yang, Z. Zhou, R. Tian, L. Lin, Y. Ma, J. Song, X. Chen, *Nat. Commun.* **2020**, *11*, 4951.

[114] B. Perillo, M. Di Donato, A. Pezone, E. Di Zazzo, P. Giovannelli, G. Galasso, G. Castoria, A. Migliaccio, *Exp. Mol. Med.* **2020**, *52*, 192.

[115] A. A. Dayem, H. Y. Choi, J. H. Kim, S. G. Cho, *Cancers* **2010**, *2*, 859.

[116] P. Ling, P. Yang, X. Gao, X. Sun, F. Gao, *J. Mater. Chem. B* **2022**, *10*, 9607.

[117] X. Zhang, X. Chen, Y. Zhao, *Nano-Micro Lett.* **2022**, *14*, 95.

[118] A. E. R. Kartikasari, C. S. Huertas, A. Mitchell, M. Plebanski, *Front. Oncol.* **2021**, *11*, 692142.

[119] a) M. Perfezou, A. Turner, A. Merkoci, *Chem. Soc. Rev.* **2012**, *41*, 2606; b) C. L. Weston, M. J. Glantz, J. R. Connor, *Fluids Barriers CNS* **2011**, *8*, 14; c) D. Sun, J. Lu, L. Zhang, Z. Chen, *Anal. Chim. Acta* **2019**, *1082*, 1; d) J. Chen, J. Li, Y. Sun, *Lab Chip* **2012**, *12*, 1753.

[120] S. Mehla, P. R. Selvakannan, M. Mazur, S. K. Bhargava, in *Additive Manufacturing for Chemical Sciences and Engineering*, Springer, Singapore **2022**, pp. 169–238.

[121] S. K. Maji, A. K. Mandal, K. T. Nguyen, P. Borah, Y. Zhao, *ACS Appl. Mater. Interfaces* **2015**, *7*, 9807.

[122] K. Fan, C. Cao, Y. Pan, D. Lu, D. Yang, J. Feng, L. Song, M. Liang, X. Yan, *Nat. Nanotechnol.* **2012**, *7*, 459.

[123] X. Zhang, F. G. Wu, P. Liu, N. Gu, Z. Chen, *Small* **2014**, *10*, 5170.

[124] Y. Liu, M. Zhou, W. Cao, X. Wang, Q. Wang, S. Li, H. Wei, *Anal. Chem.* **2019**, *91*, 8170.

[125] H. H. Pang, Y. C. Ke, N. S. Li, Y. T. Chen, C. Y. Huang, K. C. Wei, H. W. Yang, *Biosens. Bioelectron.* **2020**, *165*, 112325.

[126] Z. Wang, X. Yang, J. Feng, Y. Tang, Y. Jiang, N. He, *Analyst* **2014**, *139*, 6088.

[127] R. Bhattacharjee, S. Tanaka, S. Moriam, M. K. Masud, J. Lin, S. M. Alshehri, T. Ahamad, R. R. Salunkhe, N. T. Nguyen, Y. Yamauchi, M. S. A. Hossain, M. J. A. Shiddiky, *J. Mater. Chem. B* **2018**, *6*, 4783.

[128] J. Di, J. Price, X. Gu, X. Jiang, Y. Jing, Z. Gu, *Adv. Healthcare Mater.* **2014**, *3*, 811.

[129] J. Huang, L. Jiao, W. Xu, Q. Fang, H. Wang, X. Cai, H. Yan, W. Gu, C. Zhu, *ACS Appl. Mater. Interfaces* **2021**, *13*, 33383.

[130] C. Kang, W. Cho, M. Park, J. Kim, S. Park, D. Shin, C. Song, D. Lee, *Biomaterials* **2016**, *85*, 195.

[131] M. P. Lisanti, U. E. Martinez-Outschoorn, Z. Lin, S. Pavlides, D. Whitaker-Menezes, R. G. Pestell, A. Howell, F. Sotgia, *Cell Cycle* **2011**, *10*, 2440.

[132] F. Yang, S. Hu, Y. Zhang, X. Cai, Y. Huang, F. Wang, S. Wen, G. Teng, N. Gu, *Adv. Mater.* **2012**, *24*, 5205.

[133] F. Gong, N. Yang, Y. Wang, M. Zhuo, Q. Zhao, S. Wang, Y. Li, Z. Liu, Q. Chen, L. Cheng, *Small* **2020**, *16*, 2003496.

[134] Z. Wang, Z. Li, Z. Sun, S. Wang, Z. Ali, S. Zhu, S. Liu, Q. Ren, F. Sheng, B. Wang, Y. Hou, *Sci. Adv.* **2020**, *6*, eabc8733.

[135] S. y. Guo, D. Sun, D. l. Ni, M. r. Yu, K. Qian, W. Zhang, Y. w. Yang, S. Song, Y. Li, z. y. Xi, J. Wang, j. y. Li, Y. Wei, K. x. Chen, Y. Gan, Z. t. Wang, *Adv. Funct. Mater.* **2020**, *30*, 2000486.

[136] Y. Xing, L. Wang, L. Wang, J. Huang, S. Wang, X. Xie, J. Zhu, T. Ding, K. Cai, J. Zhang, *Adv. Funct. Mater.* **2021**, *32*, 2111171.

[137] N. V. S. Vallabani, A. S. Karakoti, S. Singh, *Colloids Surf., B* **2017**, *153*, 52.

[138] a) S. Fu, S. Wang, X. Zhang, A. Qi, Z. Liu, X. Yu, C. Chen, L. Li, *Colloids Surf., B* **2017**, *154*, 239; b) S. Yao, X. Zhao, X. Wang, T. Huang, Y. Ding, J. Zhang, Z. Zhang, Z. L. Wang, L. Li, *Adv. Mater.* **2022**, *34*,

[139] a) W. Liu, M. L. Ruan, L. Liu, X. Ji, Y. Ma, P. Yuan, G. Tang, H. Lin, J. Dai, W. Xue, *Theranostics* **2020**, *10*, 2201; b) M. Huo, L. Wang, Y. Chen, J. Shi, *Nat. Commun.* **2017**, *8*, 357.

[140] A. A. P. Mansur, H. S. Mansur, S. M. Carvalho, *Catal. Today* **2022**, *388–389*, 187.

[141] P. Wang, S. Liu, M. Hu, H. Zhang, D. Duan, J. He, J. Hong, R. Lv, H. S. Choi, X. Yan, M. Liang, *Adv. Funct. Mater.* **2020**, *30*, 2000647.

[142] Z. Xu, L. Zhang, M. Pan, Q. Jiang, Y. Huang, F. Wang, X. Liu, *Adv. Funct. Mater.* **2021**, *31*, 2104100.

[143] M. Chang, Z. Hou, M. Wang, C. Yang, R. Wang, F. Li, D. Liu, T. Peng, C. Li, J. Lin, *Angew. Chem., Int. Ed. Engl.* **2021**, *60*, 12971.

[144] Y. Zhang, Y. Wang, Q. Zhou, X. Chen, W. Jiao, G. Li, M. Peng, X. Liu, Y. He, H. Fan, *ACS Appl. Mater. Interfaces* **2021**, *13*, 52395.

[145] S. Jin, L. Weng, Z. Li, Z. Yang, L. Zhu, J. Shi, W. Tang, W. Ma, H. Zong, W. Jiang, *J. Mater. Chem. B* **2020**, *8*, 4620.

[146] D. Jana, D. Wang, A. K. Bindra, Y. Guo, J. Liu, Y. Zhao, *ACS Nano* **2021**, *15*, 7774.

[147] Y. Su, F. Wu, Q. Song, M. Wu, M. Mohammadniaei, T. Zhang, B. Liu, S. Wu, M. Zhang, A. Li, J. Shen, *Biomaterials* **2022**, *281*, 121325.

[148] X. Zhu, Y. Liu, G. Yuan, X. Guo, J. Cen, Y. Gong, J. Liu, Y. Gang, *Nanoscale* **2020**, *12*, 22317.

[149] S. Fu, R. Yang, L. Zhang, W. Liu, G. Du, Y. Cao, Z. Xu, H. Cui, Y. Kang, P. Xue, *Biomaterials* **2020**, *257*, 120279.

[150] L. Zeng, Y. Han, Z. Chen, K. Jiang, D. Golberg, Q. Weng, *Adv. Sci. (Weinh)* **2021**, *8*, 2101184.

[151] X. Li, C. Zhao, G. Deng, W. Liu, J. Shao, Z. Zhou, F. Liu, H. Yang, S. Yang, *ACS Appl. Bio Mater.* **2020**, *3*, 1769.

[152] C. Zhang, X. Wang, X. Dong, L. Mei, X. Wu, Z. Gu, Y. Zhao, *Biomaterials* **2021**, *276*, 121023.

[153] H. Wu, L. Liu, L. Song, M. Ma, N. Gu, Y. Zhang, *ACS Nano* **2019**, *13*, 14013.

[154] N. Feng, Q. Li, Q. Bai, S. Xu, J. Shi, B. Liu, J. Guo, *J. Colloid Interface Sci.* **2022**, *618*, 68.

[155] X. Zhong, X. Wang, L. Cheng, Y. a. Tang, G. Zhan, F. Gong, R. Zhang, J. Hu, Z. Liu, X. Yang, *Adv. Funct. Mater.* **2019**, *30*, 1907954.

[156] H. Ranji-Burachaloo, F. Karimi, K. Xie, Q. Fu, P. A. Gurr, D. E. Dunstan, G. G. Qiao, *ACS Appl. Mater. Interfaces* **2017**, *9*, 33599.

[157] K. Fan, J. Xi, L. Fan, P. Wang, C. Zhu, Y. Tang, X. Xu, M. Liang, B. Jiang, X. Yan, L. Gao, *Nat. Commun.* **2018**, *9*, 1440.

[158] R. Mo, Z. Gu, *Mater. Today* **2016**, *19*, 274.

[159] S. Sheng, F. Liu, L. Lin, N. Yan, Y. Wang, C. Xu, H. Tian, X. Chen, *J. Controlled Release* **2020**, *328*, 631.

[160] X. Lu, S. Gao, H. Lin, J. Shi, *Small* **2021**, *17*, 2004467.

[161] D. Zhu, H. Chen, C. Huang, G. Li, X. Wang, W. Jiang, K. Fan, *Adv. Funct. Mater.* **2022**, *32*, 2110268.

[162] M. Allinen, R. Beroukhim, L. Cai, C. Brennan, J. Lahti-Domenici, H. Huang, D. Porter, M. Hu, L. Chin, A. Richardson, S. Schnitt, W. R. Sellers, K. Polyak, *Cancer Cell* **2004**, *6*, 17.

[163] a) Y. Zhang, S. Bo, T. Feng, X. Qin, Y. Wan, S. Jiang, C. Li, J. Lin, T. Wang, X. Zhou, Z. X. Jiang, P. Huang, *Adv. Mater.* **2019**, *31*, 1806444; b) Y. Li, K. H. Yun, H. Lee, S. H. Goh, Y. G. Suh, Y. Choi, *Biomaterials* **2019**, *197*, 12; c) X. Zhou, M. You, F. Wang, Z. Wang, X. Gao, C. Jing, J. Liu, M. Guo, J. Li, A. Luo, H. Liu, Z. Liu, C. Chen, *Adv. Mater.* **2021**, *33*, 2100556.

[164] P. N. Navya, A. Kaphle, S. P. Srinivas, S. K. Bhargava, V. M. Rotello, H. K. Daima, *Nano Convergence* **2019**, *6*, 23.

[165] L. Feng, Z. Dong, C. Liang, M. Chen, D. Tao, L. Cheng, K. Yang, Z. Liu, *Biomaterials* **2018**, *181*, 81.

[166] S. Carregal-Romero, A. B. Miguel-Coello, L. Martinez-Parra, Y. Marti-Mateo, P. Hernansanz-Agustin, Y. Fernandez-Afonso, S. Plaza-Garcia, L. Gutierrez, M. D. M. Munoz-Hernandez, J. Carrillo-Romero, M. Pinol-Cancer, P. Lecante, Z. Blasco-Iturri, L. Fadon, A.

2109568; c) M. Jiang, S. Zheng, Z. Zhu, *Front. Bioeng. Biotechnol.* **2022**, *10*, 899858.

C. Almansa-Garcia, M. Moller, D. Otaegui, J. A. Enriquez, H. Groult, J. Ruiz-Cabello, *Small* **2022**, *18*, 2106570.

[167] Y. Wang, S. Song, T. Lu, Y. Cheng, Y. Song, S. Wang, F. Tan, J. Li, N. Li, *Biomaterials* **2019**, *220*, 119405.

[168] H. Cheng, D. Huo, C. Zhu, S. Shen, W. Wang, H. Li, Z. Zhu, Y. Xia, *Biomaterials* **2018**, *178*, 517.

[169] a) M. Wen, J. Ouyang, C. Wei, H. Li, W. Chen, Y. N. Liu, *Angew. Chem., Int. Ed. Engl.* **2019**, *58*, 17425; b) Z. Lv, S. He, Y. Wang, X. Zhu, *Adv. Healthcare Mater.* **2021**, *10*, 2001806.

[170] G. Liu, A. W. Robertson, M. M. Li, W. C. H. Kuo, M. T. Darby, M. H. Muhieddine, Y. C. Lin, K. Suenaga, M. Stamatakis, J. H. Warner, S. C. E. Tsang, *Nat. Chem.* **2017**, *9*, 810.

[171] D. Wang, H. Wu, S. Z. F. Phua, G. Yang, W. Qi Lim, L. Gu, C. Qian, H. Wang, Z. Guo, H. Chen, Y. Zhao, *Nat. Commun.* **2020**, *11*, 357.

[172] J. Wang, J. Sun, W. Hu, Y. Wang, T. Chou, B. Zhang, Q. Zhang, L. Ren, H. Wang, *Adv. Mater.* **2020**, *32*, 2001862.

[173] S. Li, K. Gu, H. Wang, B. Xu, H. Li, X. Shi, Z. Huang, H. Liu, *J. Am. Chem. Soc.* **2020**, *142*, 5649.

[174] C. Y. Wu, Y. H. Hsu, Y. Chen, L. C. Yang, S. C. Tseng, W. R. Chen, C. C. Huang, D. Wan, *ACS Appl. Mater. Interfaces* **2021**, *13*, 38090.

[175] D. Wang, J. Zhou, R. Shi, H. Wu, R. Chen, B. Duan, G. Xia, P. Xu, H. Wang, S. Zhou, C. Wang, H. Wang, Z. Guo, Q. Chen, *Theranostics* **2017**, *7*, 4605.

[176] H. Wang, R. Qu, Q. Chen, T. Zhang, X. Chen, B. Wu, T. Chen, *J. Mater. Chem. B* **2022**, *10*, 5410.

[177] B. Jiang, D. Duan, L. Gao, M. Zhou, K. Fan, Y. Tang, J. Xi, Y. Bi, Z. Tong, G. F. Gao, N. Xie, A. Tang, G. Nie, M. Liang, X. Yan, *Nat Protoc.* **2018**, *13*, 1506

[178] H. Huang, W. Feng, Y. Chen, J. Shi, *Nano Today* **2020**, *35*.

[179] B. Thiesen, A. Jordan, *Int. J. Hyperthermia* **2008**, *24*, 467.

[180] K. Maier-Hauff, F. Ulrich, D. Nestler, H. Niehoff, P. Wust, B. Thiesen, H. Orawa, V. Budach, A. Jordan, *J. Neurooncol.* **2011**, *103*, 317.

[181] R. Zhang, F. Kiessling, T. Lammers, R. M. Pallares, *Drug Deliv. Transl. Res.* **2023**, *13*, 378.

[182] A. R. Rastinehad, H. Anastos, E. Wajswol, J. S. Winoker, J. P. Sfakianos, S. K. Doppalapudi, M. R. Carrick, C. J. Knauer, B. Taouli, S. C. Lewis, A. K. Tewari, J. A. Schwartz, S. E. Canfield, A. K. George, J. L. West, N. J. Halas, *Proc. Natl. Acad. Sci. USA* **2019**, *116*, 18590.

[183] S. K. Libutti, G. F. Paciotti, A. A. Byrnes, H. R. Alexander, Jr. W. E. Gannon, M. Walker, G. D. Seidel, N. Yuldasheva, L. Tamarkin, *Clin. Cancer Res.* **2010**, *16*, 6139.

[184] P. Kumthekar, C. H. Ko, T. Paunesku, K. Dixit, A. M. Sonabend, O. Bloch, M. Tate, M. Schwartz, L. Zuckerman, R. Lezon, R. V. Lukas, B. Jovanovic, K. McCortney, H. Colman, S. Chen, B. Lai, O. Antipova, J. Deng, L. Li, S. Tommasini-Ghelfi, L. A. Hurley, D. Unruh, N. V. Sharma, M. Kandpal, F. M. Kouri, R. V. Davuluri, D. J. Brat, M. Muzzio, M. Glass, V. Vijayakumar, et al., *Sci. Transl. Medi.* **2021**, *13*, eabb3945

[185] L. Sancey, F. Lux, S. Kotb, S. Roux, S. Dufort, A. Bianchi, Y. Cremillieux, P. Fries, J. L. Coll, C. Rodriguez-Lafrasse, M. Janier, M. Dutreix, M. Barberi-Heyob, F. Boschetti, F. Denat, C. Louis, E. Porcel, S. Lacombe, G. Le Duc, E. Deutsch, J. L. Perfettini, A. Detappe, C. Verry, R. Berbeco, K. T. Butterworth, S. J. McMahon, K. M. Prise, P. Perriat, O. Tillement, *Br. J. Radiol.* **2014**, *87*, 20140134.

[186] F. T. V. Lux, E. Thomas, S. Dufort, F. Rossetti, M. Martini, et al., *Br. J. Radiol* **2019**, *92*, 20180365.

[187] S. Bonvalot, P. L. Rutkowski, J. Thariat, S. Carrere, A. Ducassou, M. P. Sunyach, P. Agoston, A. Hong, A. Mervoyer, M. Rastrelli, V. Moreno, R. K. Li, B. Tiangco, A. C. Herraez, A. Gronchi, L. Mangel, T. Sy-Ortin, P. Hohenberger, T. de Baere, A. Le Cesne, S. Helfre, E. Saada-Bouzid, A. Borkowska, R. Anghel, A. Co, M. Gebhart, G. Kantor, A. Montero, H. H. Loong, R. Verges, et al., *Lancet. Oncol.* **2019**, *20*, 1148.

[188] S. Malola, P. Nieminen, A. Pihlajamäki, J. Hämäläinen, T. Kärkkäinen, H. Häkkinen, *Nat. Commun.* **2019**, *10*, 3973.

[189] Y. Yao, R. Zhang, T. Liu, H. Yu, G. Lu, *Inorg. Chem. Commun.* **2019**, *101*, 160.

[190] V. Negri, J. Pacheco-Torres, D. Calle, P. López-Larrubia, in *Surface-modified Nanobiomaterials for Electrochemical and Biomedicine Applications*, (Eds: A. R. Puente-Santiago, D. Rodríguez-Padrón), Springer International Publishing, Cham **2020**.

[191] X. Du, S. Z. Qiao, *Small* **2015**, *11*, 392.

[192] Y. Guo, L. S. de Vasconcelos, N. Manohar, J. Geng, K. P. Johnston, G. Yu, *Angew. Chem. Int. Ed.* **2022**, *61*, 2114074.

[193] Y. Feng, Z. Zhu, W. Chen, P. Prabakaran, K. Lin, D. S. Dimitrov, *Biomedicines* **2014**, *2*, 1.

[194] F. Rommasi, N. Esfandiari, *Nanoscale Res. Lett.* **2021**, *16*, 95.

[195] M. I. Anik, N. Mahmud, A. Al Masud, M. Hasan, *Nano Select* **2022**, *3*, 792.

[196] L. Vigderman, B. P. Khanal, E. R. Zubarev, *Adv. Mater.* **2012**, *24*, 4811.

[197] C. Kuttner, M. Mayer, M. Dulle, A. Moscoso, J. M. Lopez-Romero, S. Foŕster, A. Fery, J. Peŕez-Juste, R. Contreras-Caćeres, *ACS Appl. Mater. Interfaces* **2018**, *10*, 11152.

[198] Y. Lu, H. Zhang, F. Wu, H. Liu, J. Fang, *RSC Adv.* **2017**, *7*, 18601.

[199] Y. Sun, L. Wang, X. Yu, K. Chen, *Cryst. Eng. Comm.* **2012**, *14*, 3199.

[200] Q. Zhang, W. Li, L. P. Wen, J. Chen, Y. Xia, *Chem.–A Euro. J.* **2010**, *16*, 10234.

Navya P. N. is currently a higher degree research candidate at RMIT University, Melbourne, Australia. Prior to this, she was an assistant professor at Bannari Amman Institute of Technology, and Siddaganga Institute of Technology, India. She holds an M.Tech. degree from Manipal University, India. Her research interest is in development of biocompatible nanoparticles with suitable functionalization for a range of biomedical applications. She has published several research papers in reputed journals and is a co-editor of three books published by Springer Nature.

Sunil Mehla is an emerging early career researcher under the mentorship of Prof. Bhargava at the RMIT Centre for Advanced Materials and Industrial Chemistry. He applies additive manufacturing and nanofabrication technologies to resolve scientific and technological challenges. He studied chemistry at IIT Kanpur and chemical engineering with a specialization in catalysis at IIT Madras. He received his Ph.D. degree from RMIT University, Melbourne, in 2022 where he designed and fabricated gold microelectrode arrays for SERS-based chemical sensing. His research interests include additive manufacturing and nanofabrication, plasmonics, electrochemistry, nanomaterials, porous crystalline frameworks, and thin films.

Amrin Begum is currently pursuing a Ph.D. in applied chemistry from RMIT University, Melbourne. Her research interest is in the development of novel metal-based compounds as chemotherapeutic agents for treating cancers. She has worked as a teaching assistant at the University of Technology Sydney teaching medicinal and organic chemistry subjects. She has worked as a research assistant at the Indian Institute of Chemical Technology in India on the development of lipid based novel adjuvants.

Harit K. Chaturvedi is the chairman and head surgical oncologist at the Max Institute of Cancer Care (MICC). He joined MICC in 2009 and built India's largest and finest oncology programs. He has developed his team of over a hundred oncologistsand built a Disease Management Group (DMG) model. He has performed surgeries at live surgical workshops, presented his work at conferences, and has published in peer-reviewed journals. He has served the national bodies, viz, Indian Society of Oncology and Indian Association of Surgical Oncology as president. He has built the brand of the Indian Cancer Congress as its first organizing secretary.

Ruchika Ojha is a Vice-Chancellor's Research Fellow in the School of Science at RMIT University. She is a Molecular Engineering Group leader at the Centre of Advanced Materials and Industrial Chemistry Her research interests include synthesizing advanced materials such as gold and platinum anti-cancer agents, solution and solid-state electrochemical analysis, generation and stabilization of the metal complexes with rare oxidation states, activated carbon materials, hydrogen storage, and energy-storage systems.

Christian Hartinger was appointed at the University of Auckland in 2011 where he was promoted to professor in 2016. He is currently the secretary of the Society of Biological Inorganic Chemistry (SBIC). Prof. Hartinger has published more than 230 peer-reviewed papers in journals such as *Angewandte Chemie*, *Chemical Science*, *Chemical Reviews*, *Coordination Chemistry Reviews*, *Journal of Medicinal Chemistry*, *ChemComm*, *Inorganic Chemistry*, etc. His papers have been cited over 15 500 times, his Scopus h-index is 69, and he is a regular plenary and keynote speaker at conferences. Prof. Hartinger is the recipient of many national and international awards.

Magdalena Plebanski is a Ph.D. (immunology), M.B.A. (business), D.P.S. (psychology), B.Sc.Hon. (virology), and NHMRC senior research fellow. She develops new immune-based therapies and vaccines to optimize vaccination for the elderly, and to develop new diagnostics, prognostics, and treatments for ovarian cancer, together with universities, hospitals and pharma. Her >220 publications cited over 15 000 times include field- changing findings published in top journals such as *Science*, *Nature*, *Nature Biotechnology*, *Immunity*, *Nature Medicine*, *Plos Pathogens*, *PNAS*, *Nature Communications*, and *The Lancet*. Her team leads research across 20 hospitals across Australia in multiple Phase II human clinical trials, some of them underpinned by her recent patented biomarker technologies.

Suresh K. Bhargava, Ph.D., D.Sc., is the founding director of the Centre for Advanced Materials and Industrial Chemistry at RMIT University. With an h-index of 81, over 700 research articles, 15 book chapters, and 22 800 citations, he has made major technological breakthroughs in industrial chemistry, molecular engineering, nanomaterials for biomedical applications, electrochemistry, and additive manufacturing for catalysis. His contributions to science have been recognized with several awards. He is a fellow of seven academies. In 2022 he was honored as a Member of the Order of Australia for his outstanding contributions to tertiary education and Australia–India relations.